REPORT NO. GDCA 632-3-140
CONTRACT NAS8-27566

# DESIGN AND DEVELOPMENT OF POLYPHENYLENE OXIDE FOAM AS A REUSABLE INTERNAL INSULATION FOR $LH_2$ TANKS

PHASE TWO PROGRESS REPORT

GENERAL DYNAMICS
Convair Aerospace Division

REPORT NO. GDCA 632-3-140
CONTRACT NAS 8-27566

# DESIGN AND DEVELOPMENT OF POLYPHENYLENE OXIDE FOAM AS A REUSABLE INTERNAL INSULATION FOR $LH_2$ TANKS

PHASE TWO PROGRESS REPORT

15 September 1972

Submitted to
National Aeronautics and Space Administration
GEORGE C. MARSHALL SPACE FLIGHT CENTER
Huntsville, Alabama

Prepared by
CONVAIR AEROSPACE DIVISION OF GENERAL DYNAMICS
San Diego, California

## ABSTRACT

Under Contract NAS8-27566, "Design and Development of Polyphenylene Oxide Foam as a Reusable Insulation for $LH_2$ Tanks," PPO foam has been tested for mechanical strength, for the effects of 100 thermal cycles from 450K (350F) to 21K (-423F) and for gas flow resistance characteristics. PPO foam panels have been investigated for density variations, methods for joining panels have been studied and panel joint thermal test specimens have been fabricated. The range of foam panel thicknesses under investigation has been extended to include 7 mm (0.3 in) and 70 mm (2.8 in) panels which have also been tested for thermal performance.

## FOREWORD

This report describes the work done by the Convair Aerospace Division of General Dynamics during Phase One of Contract NAS8-27566. The work was administered under the technical direction of Mr. L. M. Thompson, S&E-ASTN-MNM, Astronautics Laboratory of the George C. Marshall Space Flight Center.

In addition to the project leader, R. E. Tatro, the following Convair Aerospace personnel made contributions to the study:

| | |
|---|---|
| F. O. Bennett | Thermodynamics |
| H. G. Brittain | Engineering Test |
| R. C. Day | Thermodynamics |
| B. G. Ganoe | Engineering Test |
| C. F. Johnson | Engineering Test |
| L. C. May | Materials Research |
| P. Merz | Materials Research |
| R. L. Otwell | Thermodynamics |
| M. Podell | Materials Research |
| C. Snyder | Manufacturing Development |
| G. B. Yates | Thermodynamics |

TABLE OF CONTENTS

LIST OF ILLUSTRATIONS

LIST OF ILLUSTRATIONS, Contd

LIST OF TABLES

## SUMMARY

Results are presented for the work accomplished during the phase two reporting period under Contract NAS8-27566, "Design and Development of Polyphenylene Oxide Foam as a Reusable Internal Insulation for $LH_2$ Tanks." Work included the determination of density variations in PPO foam panels from the 1972 master order of 72 panels. Foam from these panels was also tested for the effects of 100 temperature cycles from 21K (-423F) to 450K (350F), for gas flow resistance characteristics and for mechanical strength at 21K (-423F), 294K (70F) and 423K (300F). Methods of joining panels have been investigated. The results of the panel x-ray inspection, gas flow resistance tests and density variation measurements have been correlated with the results of thermal conductivity tests. Also, the range of foam panel thicknesses under investigation has been extended to include 7 mm (0.3 in) and 70 mm (2.8 in) panels.

# SECTION 1

# INTRODUCTION

The objective of this program is to develop information on polyphenylene oxide (PPO) foam and supporting materials which will provide a competitive internal insulation system for use with reusable liquid hydrogen propellant tanks. The system must not be adversely affected by the various phases of the Space Shuttle mission cycle, must be capable of withstanding short-term exposure to a 450K (350F) environment, and must be reusable for up to 100 flights with minimum refurbishment.

To achieve this objective a two-part program, Figure 1-1, is in progress to investigate the physical and mechanical properties of various PPO foam configurations, to evaluate candidate adhesives and closeout materials for use with the foam, and to develop techniques for applying the insulation system to a cryogenic propellant tank. The results of these activities will be combined into a series of specifications ranging from required physical and mechanical characteristics of ordered materials through repair procedures for an installed insulation system.

An evaluation has been made of new PPO foam compositions produced by TNO in Delft, Holland. This evaluation task resulted from the efforts of the vendor, Lonza, Ltd. in Basle, Switzerland, to continue to improve the quality of the foam and was to permit the selection of an optimum composition which would then be used for the master order of 72 panels (Ref. 1). The panels received in 1972 have been logged in as 72-X in the order in which they arrive. The vendor has been varying the blowing agent, the nucleating agent, and the millsheet manufacturing method, and evaluating the results qualitatively, and GD/CA has been performing detailed qualitative and quantitative evaluation on the better panels. Combinations of dichloroethane (DCE), trichloroethane (CNU), and petroleum ether (SBP) have been used as blowing agents with and without the addition of vermiculite (VER) and Genitron (GEN) nucleating agents. The panels used to determine material thermal conductivity were subsequently subjected to pressure drop (permeability) and density gradient evaluations to provide complete information on specific foam samples. Based on a review of the data and discussions with the vendor, a preferred composition has been selected. For the 72- panels, plus the additional panels required for quality control, the blowing agent used was a 1:3 mixture of dichloroethane (DCE) and Chlorothene Nu (CNU), and the nucleating agent was Genitron AC/2 azodicarbonamide added in the ratio of two parts per hundred parts of resin. The panels were blown from rolled millsheets. This combination of blowing and nucleating agents was found to result in panels having the most uniform internal structure as well as low thermal conductivity. The rolled millsheet manufacturing method was chosen primarily due to the fact that, to date, the extrusion or injection molding methods have not been refined to the point where panels of high uniformity can be consistently produced.

Although the English system of units (ft, lb, sec) has been used for all measurements and calculations, in this report the S.I. (m, kg, sec) system of units is shown as the primary system with English units following in parentheses.

Figure 1-1. Program Schedule

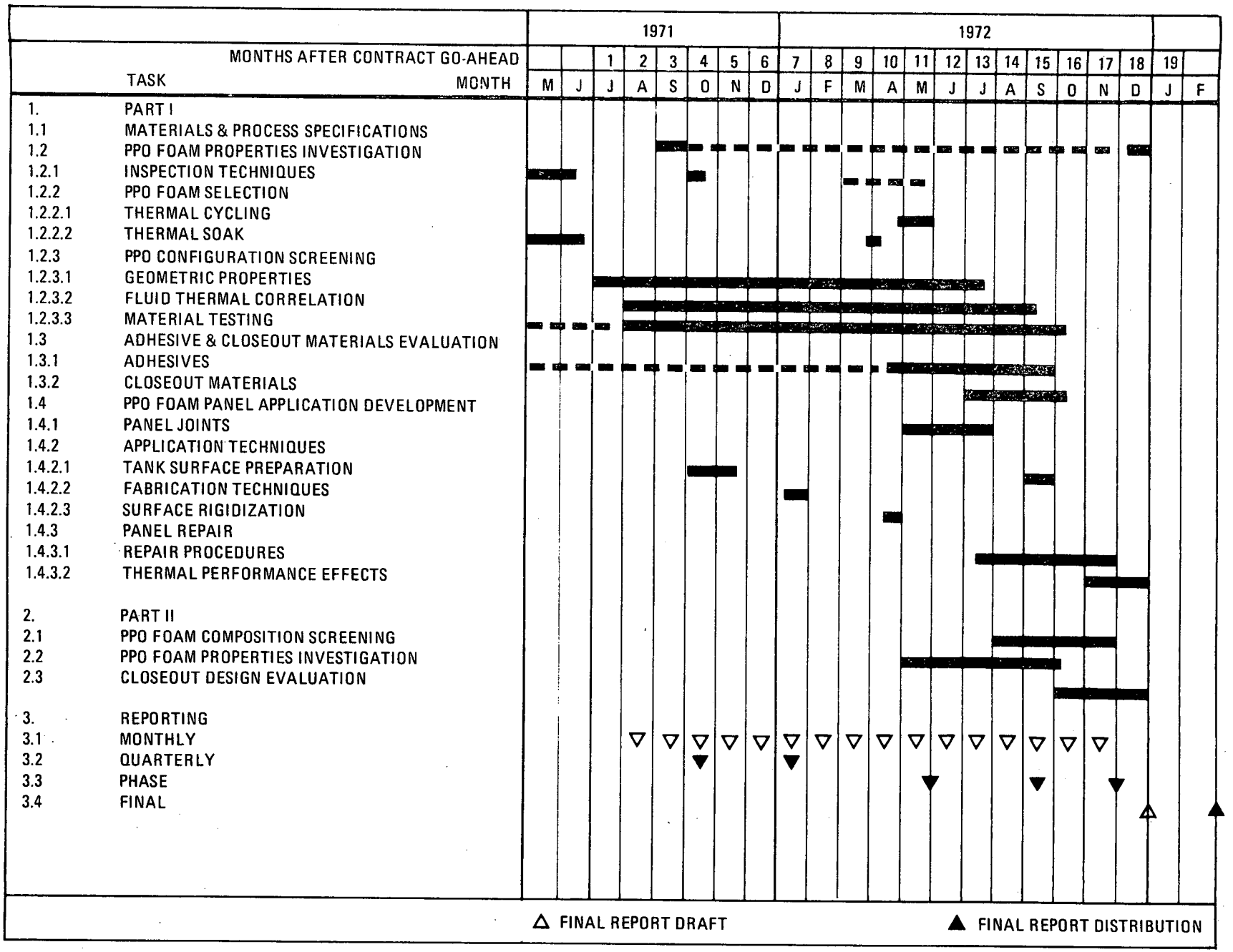

## SECTION 2

## THERMAL CYCLING (1.2.2.1)

Samples of PPO foam have been subjected to 100 temperature cycles from 21 to 450K (-423 to 350F) simulating the Space Shuttle life cycle. A cutaway drawing of the apparatus used for this test is shown in Figure 2-1. The nine 2.54 cm (1.00 in.) diameter by 2.54 cm (1.00 in.) thick PPO foam specimens were held in a copper can suspended from the positioning rod. The positioning rod, which passes through a seal at the top of the chimney, allows the specimen can to be held in the $LH_2$ bath, the heater or the lower section of the chimney. The chimney insulates the electric heater from the $LH_2$ bath by means of gas stratification. Thermocouples were located on the heater, in the center of the stack of foam specimens and at the outer surface of the specimens (see Figure 2-1). The cryostat insulates the $LH_2$ bath by means of a vacuum jacket, an $LN_2$ guard and external insulation. The foam specimens were placed in the specimen can, evacuated and helium backfilled, and maintained in an $O_2$ free atmosphere prior to placement into the cycling apparatus. A view of the thermal cycling test setup is shown in Figure 2-2.

A typical temperature cycle is shown in Figure 2-3. The test procedure for the 100 temperature cycles follows below.

### Procedure for Temperature Cycling of PPO Foam

1. Raise specimen can into heater.

2. Turn heater power on (52V).

3. When specimens are heated to 450K (+350F), turn heater off and lower specimen can to halfway position.

4. When specimen temperature has dropped to 340K (+150F), lower the specimen can into the $LH_2$.

5. After the specimen can has been in the $LH_2$ bath for 5 minutes, raise the specimen can to the halfway position.

6. When the specimen temperature reaches 200K (-100F), raise the specimen can into the heater.

7. Turn heater power on (52V).

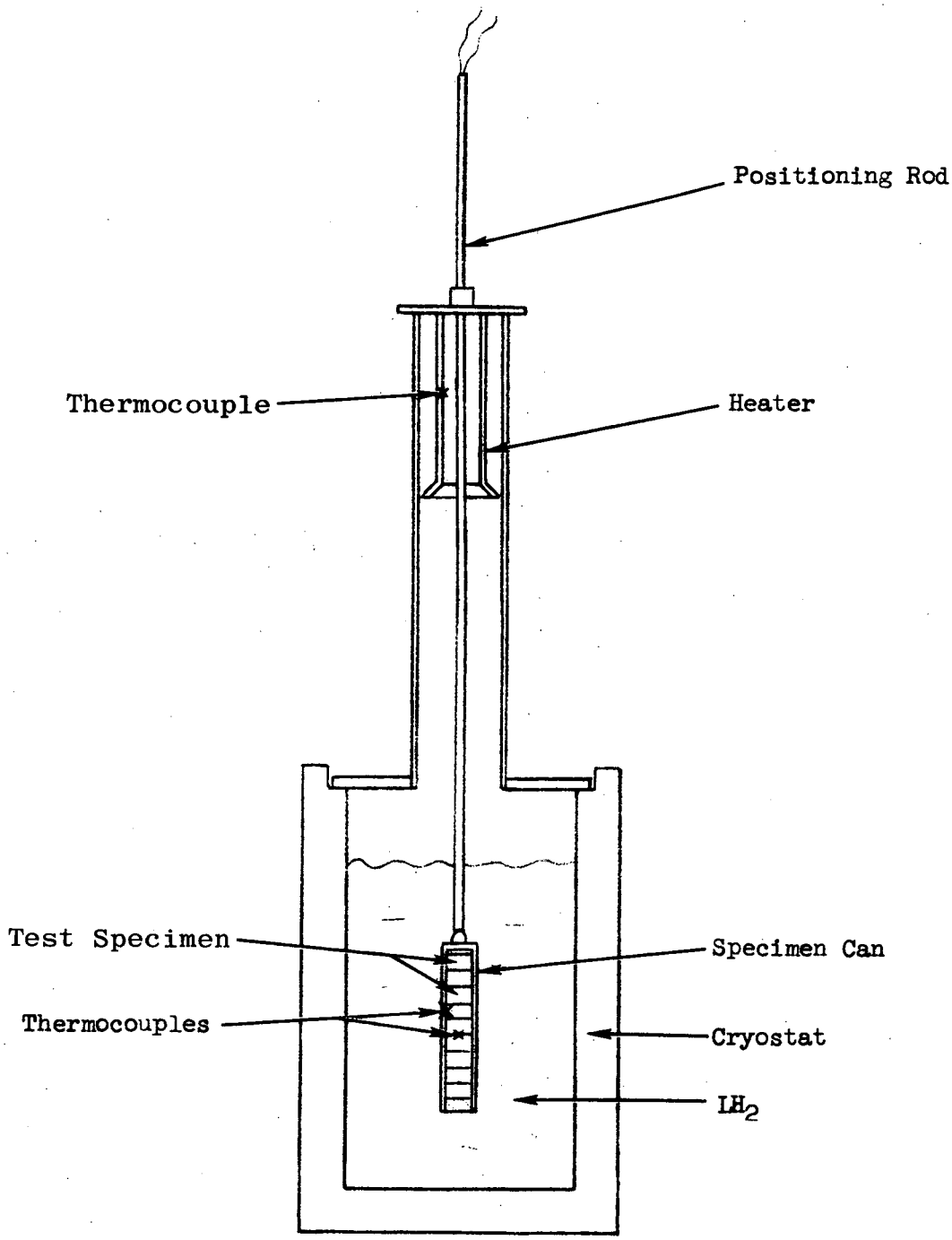


Figure 2-1. Thermal Cycling Apparatus

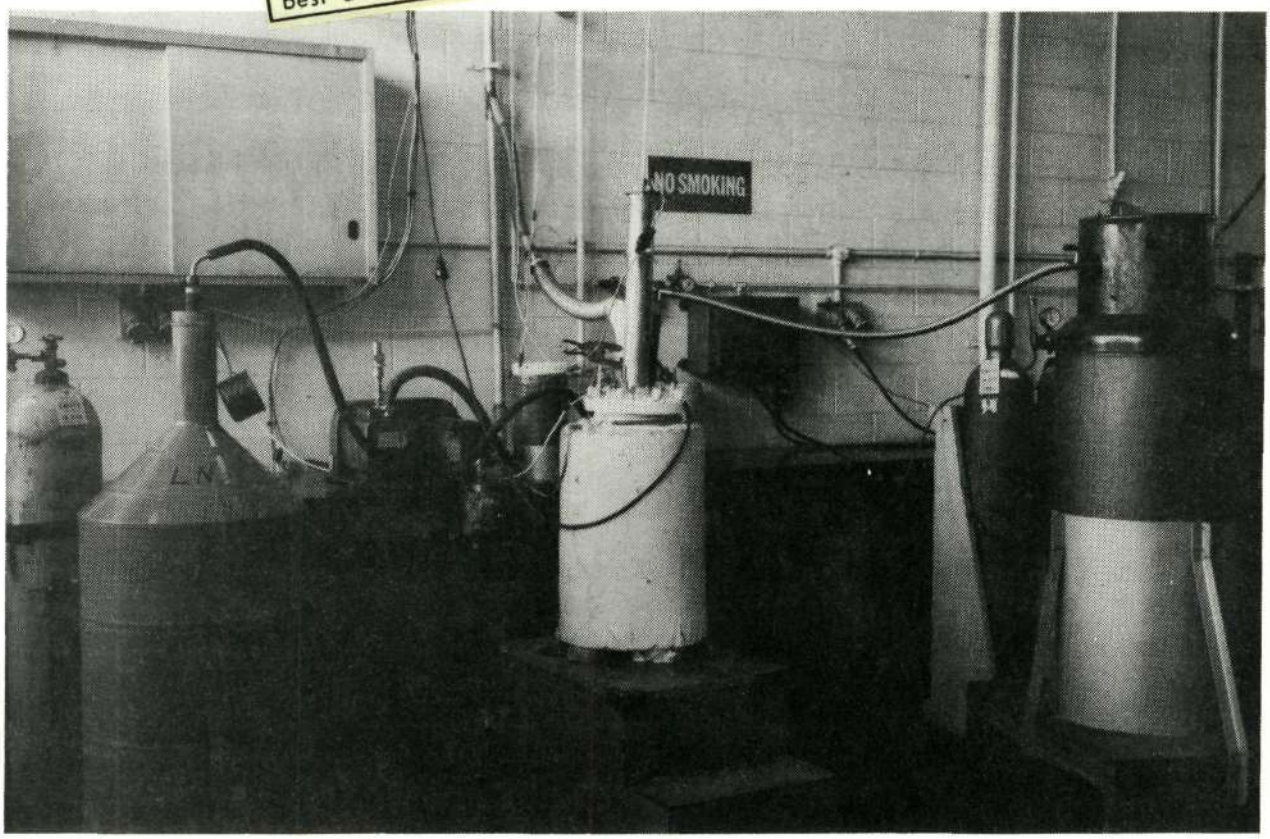


Figure 2-2. PPO Foam Thermal Cycling Test Setup

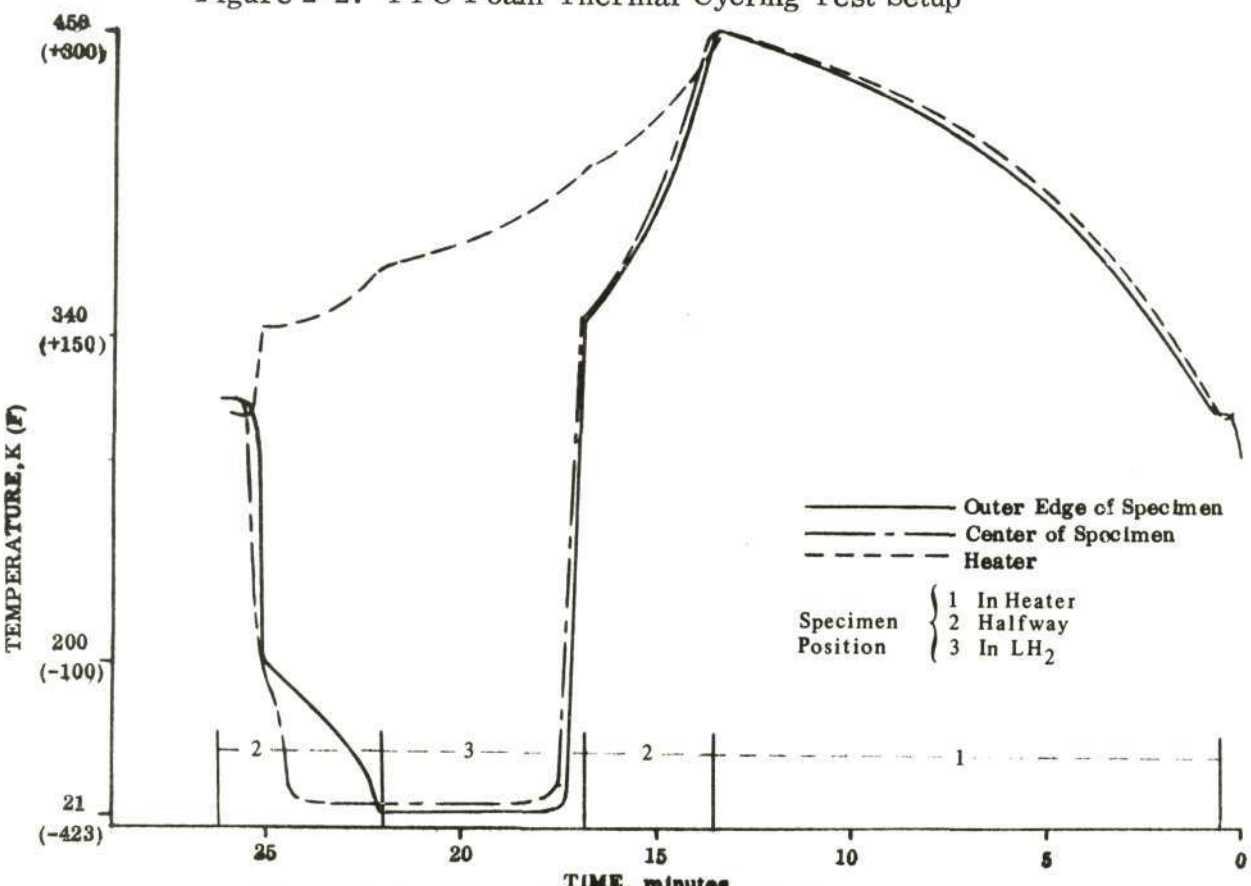


Figure 2-3. Typical PPO Foam Thermal Cycle

After completion of the 100 thermal cycles, the foam specimens were microscopically inspected for evidence of thermal aging. The only signs of thermal aging were the darkening of some of the bubbles in the cell walls and an ever so slight darkening in the general appearance of the foam (see Ref. 2). There was no visible change in cell structure. The weight of the specimens decreased by 3.7% and they shrank 1% in length (along the cells) and 0.4% in diameter (perpendicular to the cells). Longitudinal compressive strength tests were then carried out on the nine PPO foam specimens; three at 21K (-423F), three at 294K (70F) and three at 423K (300F). The results of these strength tests are shown in Figure 2-4 along with similar results obtained using virgin foam. All of the foam specimens, including the virgin material, were taken from the same PPO foam panel. Comparison of the strength data for the virgin and thermally cycled specimens shows no evidence of degradation within the normal scatter of the strength data.

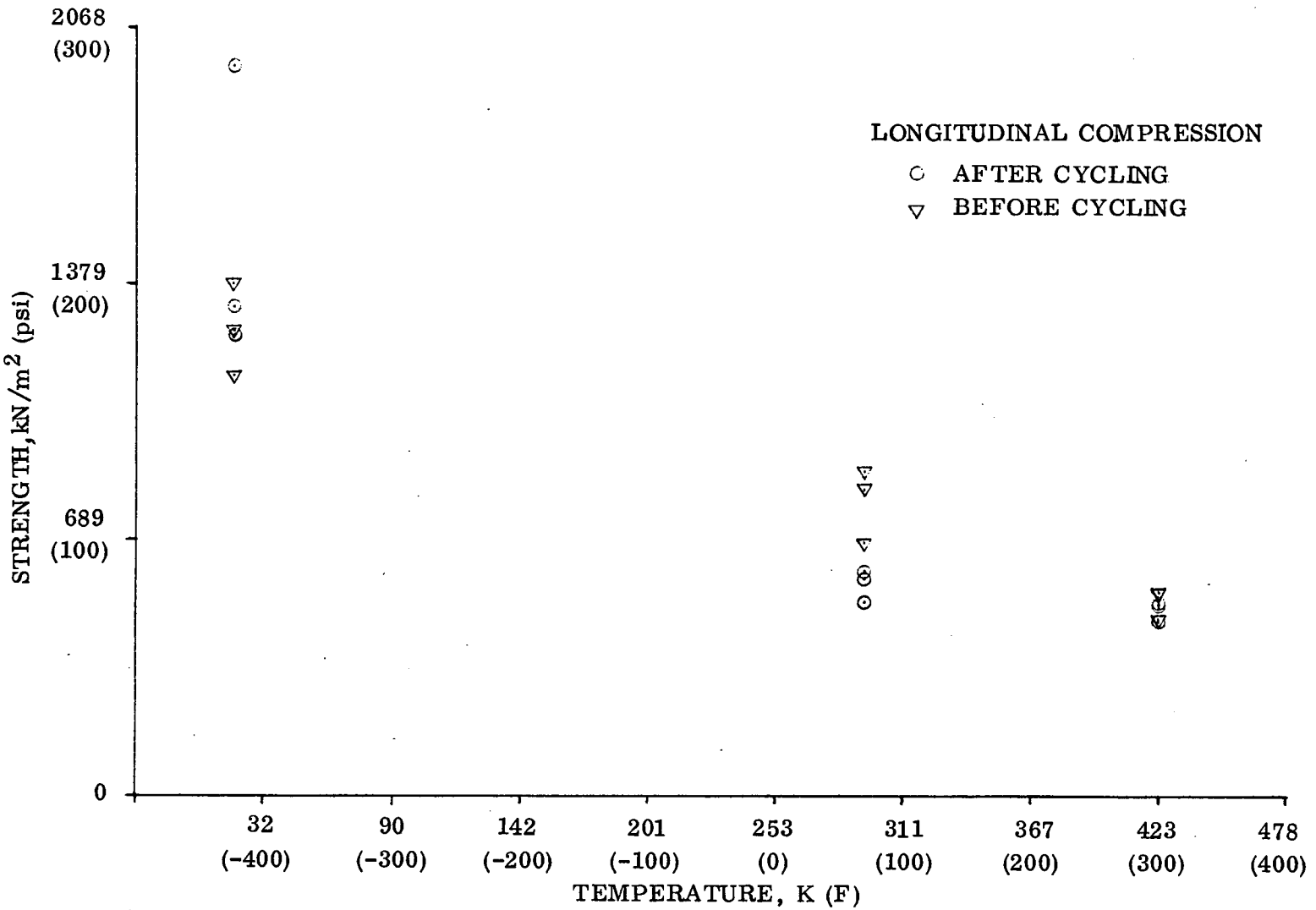


Figure 2-4. PPO Foam Thermal Cycling Strength Test Results

## SECTION 3

## GEOMETRIC PROPERTIES (1.1.2.3.1)

One of the parameters which is useful in the evaluation of the internal structural characteristics of PPO foam is the material permeability. Permeability measurements could be used together with mechanical strength and thermal conductivity data to screen different foam configurations and predict structural and thermal performance in an actual tank usage situation. Theoretically a good open cell insulation material should have a high permeability in the direction parallel to the cell orientation and a low permeability laterally. A low lateral permeability will curtail convection currents in the tank sidewall insulation while a high parallel permeability will reduce the chance of insulation failure due to pressure changes in the tank. An attempt to correlate permeability test data with the thermal performance of similar specimens will be made.

The technique used to evaluate permeability is the measurement of the internal resistance of the material to gas flow, determined by recording pressure drop through the material as a function of gas flow rate, both parallel (longitudinal) and perpendicular (lateral) to the cell orientation. Detailed analysis of this data for different foam configurations can lead to conclusions about the relative bulk densities, the comparative number of blocked cells, the extent of cell interconnections, and the relative mean cell diameters. If this information can be correlated with thermal and mechanical strength data, the material configuration can be adequately characterized with respect to its adaptability to specific use situations, and the effects of variations in the internal structure on material strength and thermal performance can be predicted.

The apparatus for testing PPO foam specimens in the perpendicular direction is illustrated in Figure 3-1. This apparatus consists of three aluminum plates with very soft rubber bonded to one side. The 88.9 mm (3.50 in.) by 44.5 mm (1.75 in.) foam specimen is bonded, with silicone rubber, between Plexiglas plates, Figure 3-2, and is then clamped between the top and bottom plates of the test apparatus. Then the end plate, with fittings for the manometer and inlet, is mounted.

Two apparatus were used to test PPO foam specimens in the parallel direction. The first, illustrated in Figure 3-3, utilized 14.1 cm (5.55 in.) diameter foam discs as specimens. The cylindrical test beaker was fabricated from 6.35 mm (0.25 in.) thick Plexiglas plate. Very soft (15-30 Durometer) silicone rubber seals are used to prevent leakage around the test specimen. The test specimen is held in place with a section of tubing weighted down with about 9 kg (20 lbs) of lead. A taper at the top of the beaker is required to allow the specimen to be placed in the beaker with ease since PPO foam specimens are about 1.27 mm (0.050 in.) oversize. To remove a specimen, the plug at the bottom of the beaker is removed and the plate in the bottom of the beaker is forced against the specimen with a rod.

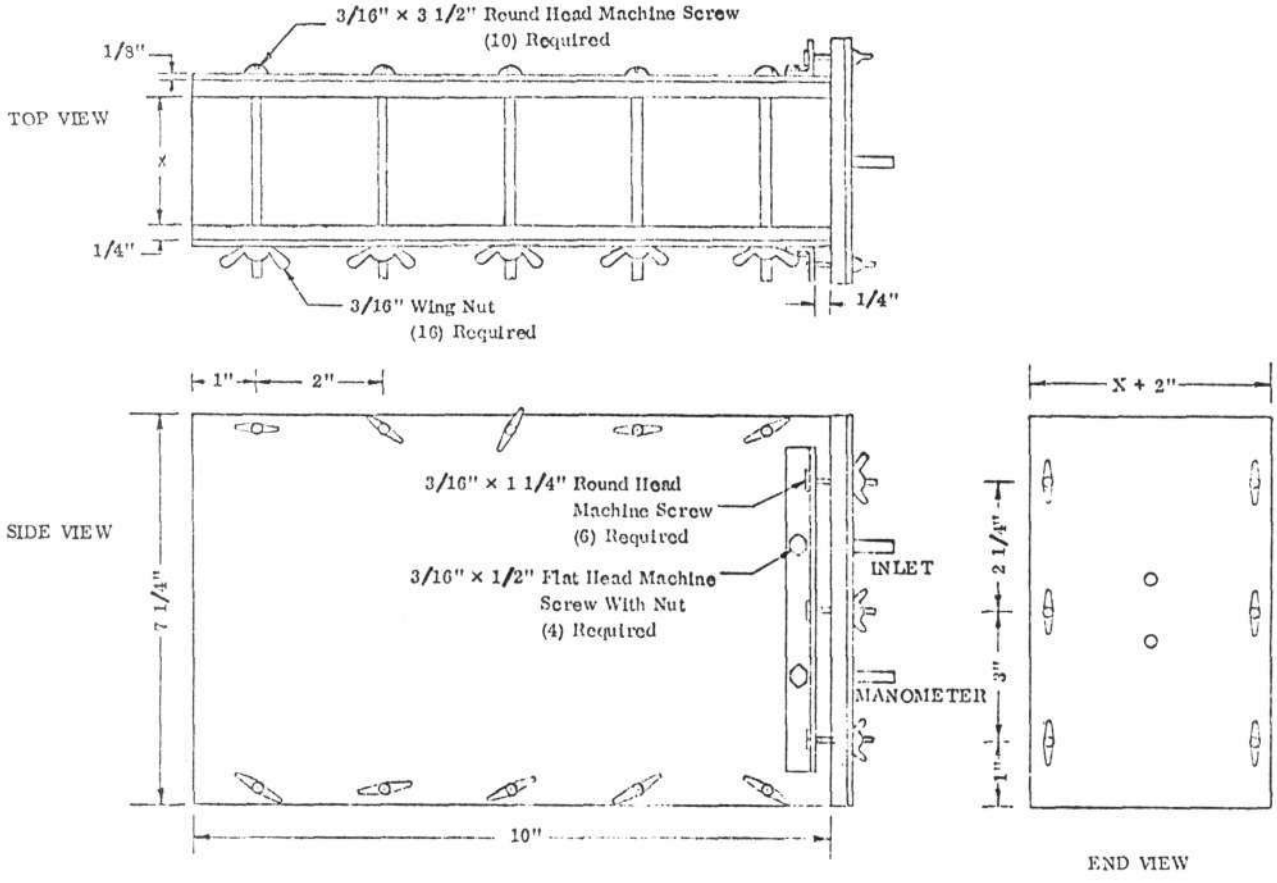


Figure 3-1. Perpendicular Gas Flow Resistance Apparatus

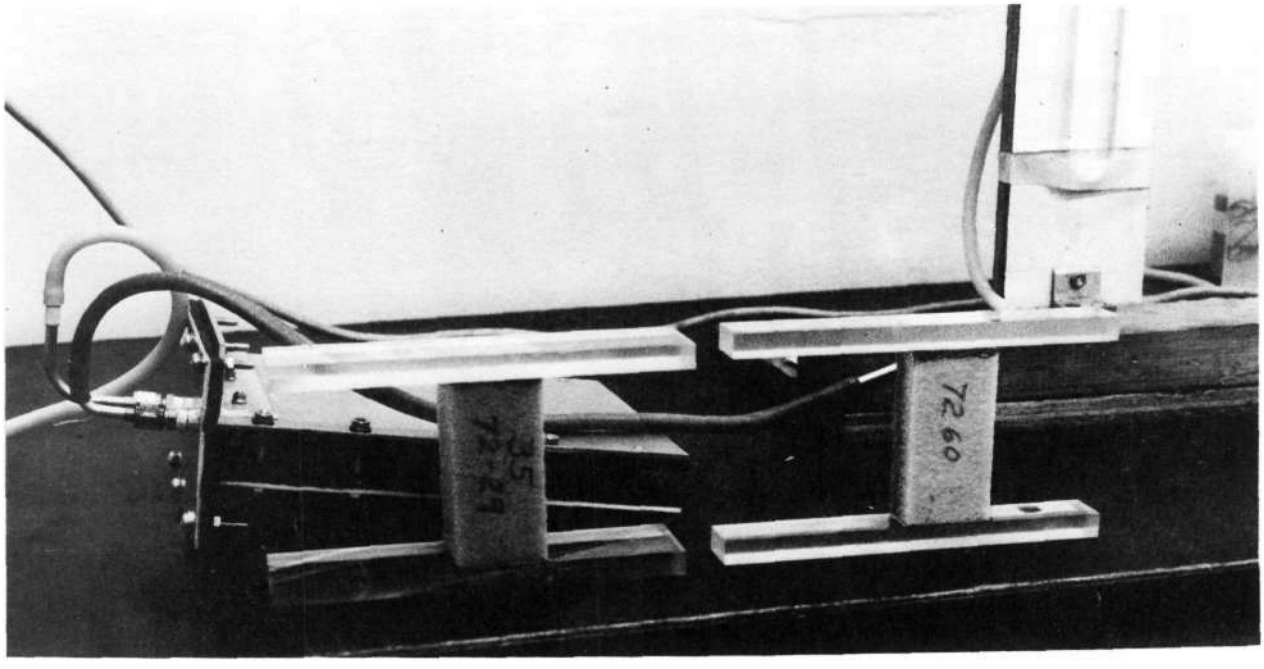


Figure 3-2. Specimens Prepared for Perpendicular Gas Flow Resistance Test

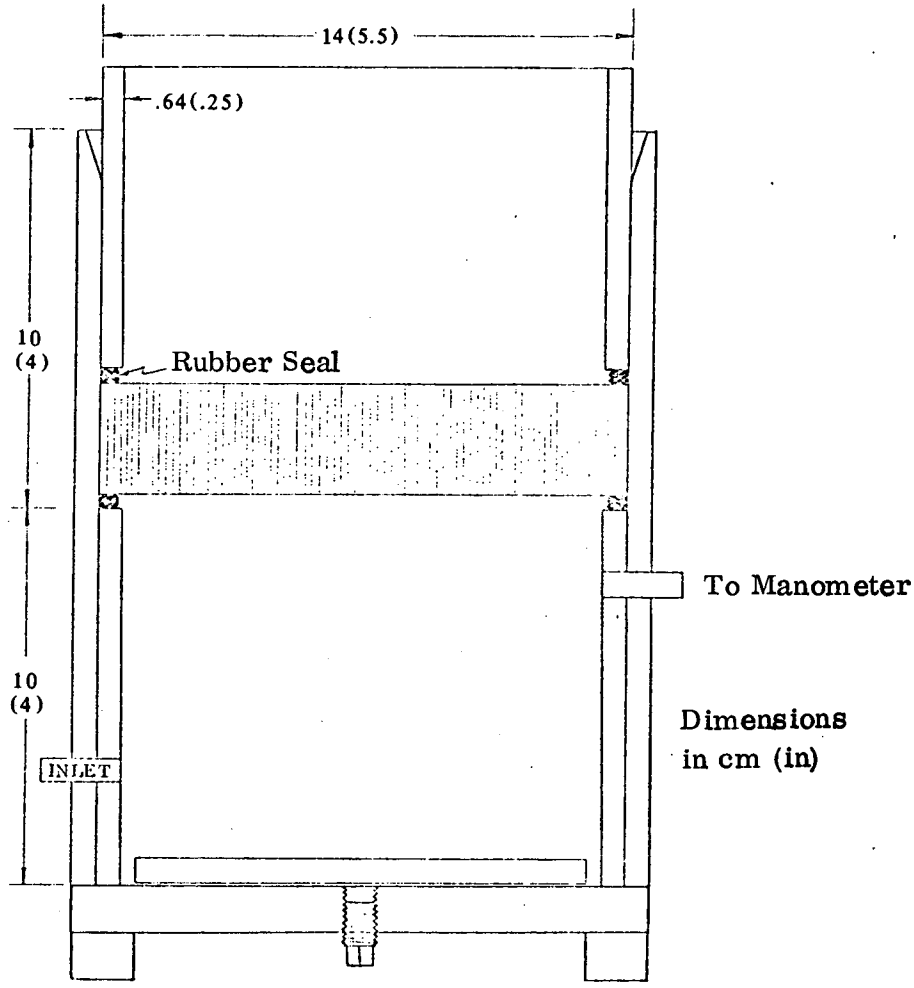


Figure 3-3. Cylindrical Beaker Parallel Gas Flow Resistance Apparatus

The second parallel flow apparatus, illustrated in Figure 3-4, was designed to allow both parallel and perpendicular flow tests on the same piece of foam. After testing in the perpendicular flow apparatus, Figure 3-2, the Plexiglas side plates are trimmed even with the foam block and then the remaining pieces of the side plates are bonded, with silicone rubber, to the 88.9 mm (3.50 in.) faces of the foam block, see Figure 3-5. The test specimen is then placed on top of the test apparatus and is compressed, by lead weights, against a soft rubber seal bonded to the top rim of the rectangular beaker. Thus, a positive seal is established between the beaker and the Plexiglas frame around the foam, avoiding any crushing of the foam specimen.

A schematic of the gas flow resistance test setup is shown in Figure 3-6. The bleed valve allows the gas supply regulator valve to operate stably at a high flow rate, while the flow to the test apparatus is quite low. The multiple tube flowmeter and the

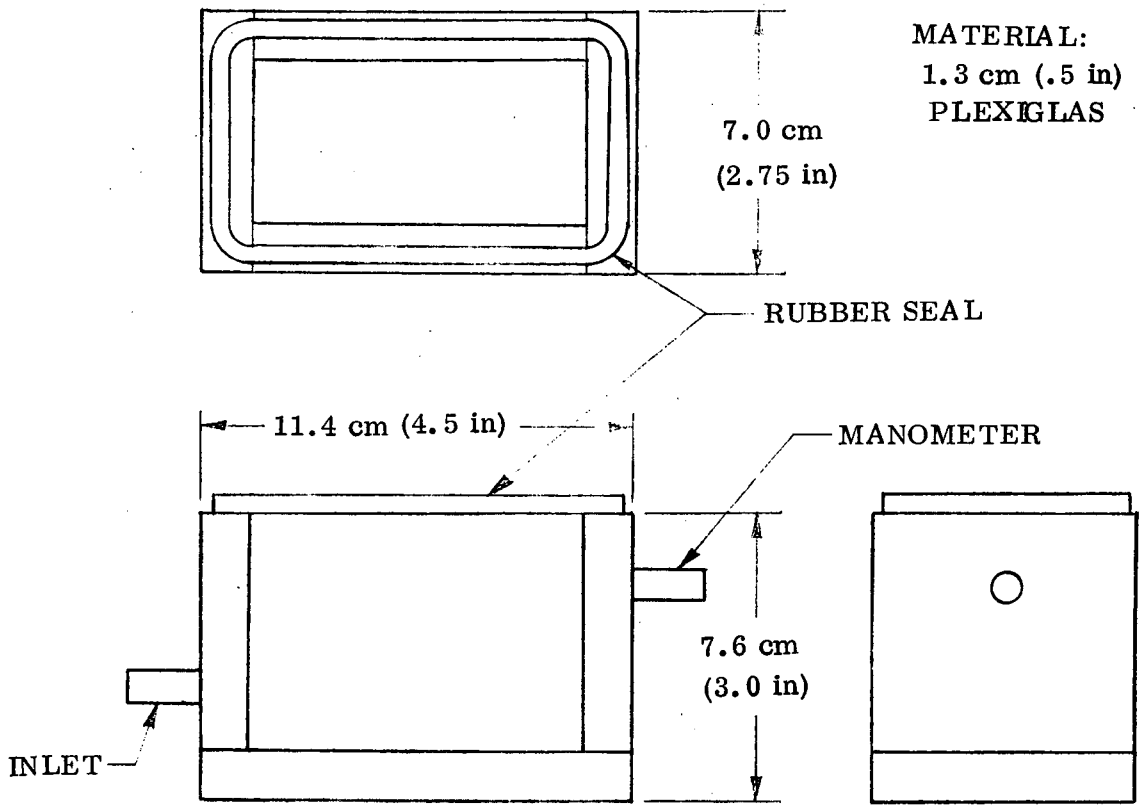


Figure 3-4. Square Beaker Parallel Gas Flow Resistance Apparatus

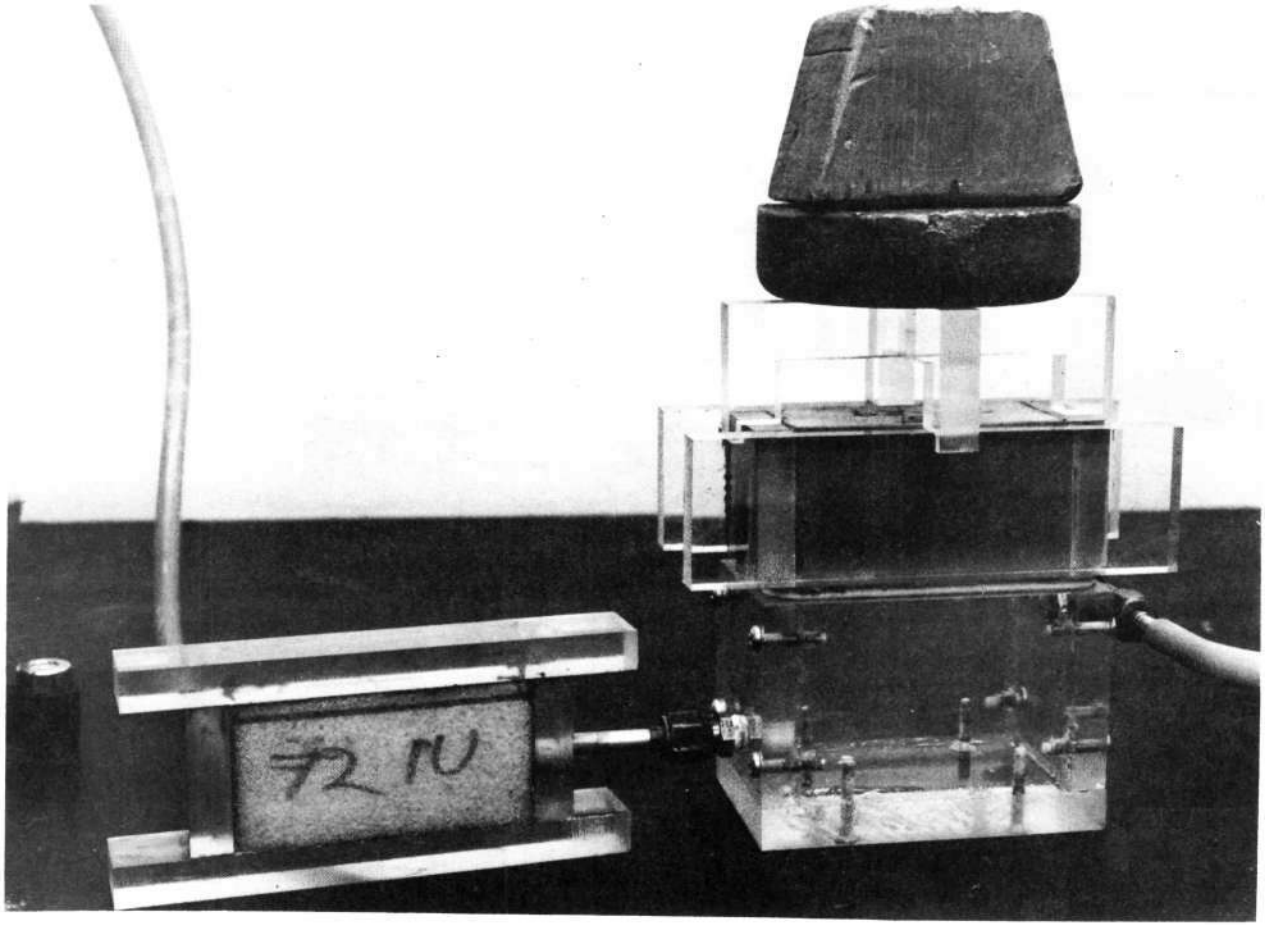


Figure 3-5. Specimen Prepared for Parallel Gas Flow Resistance

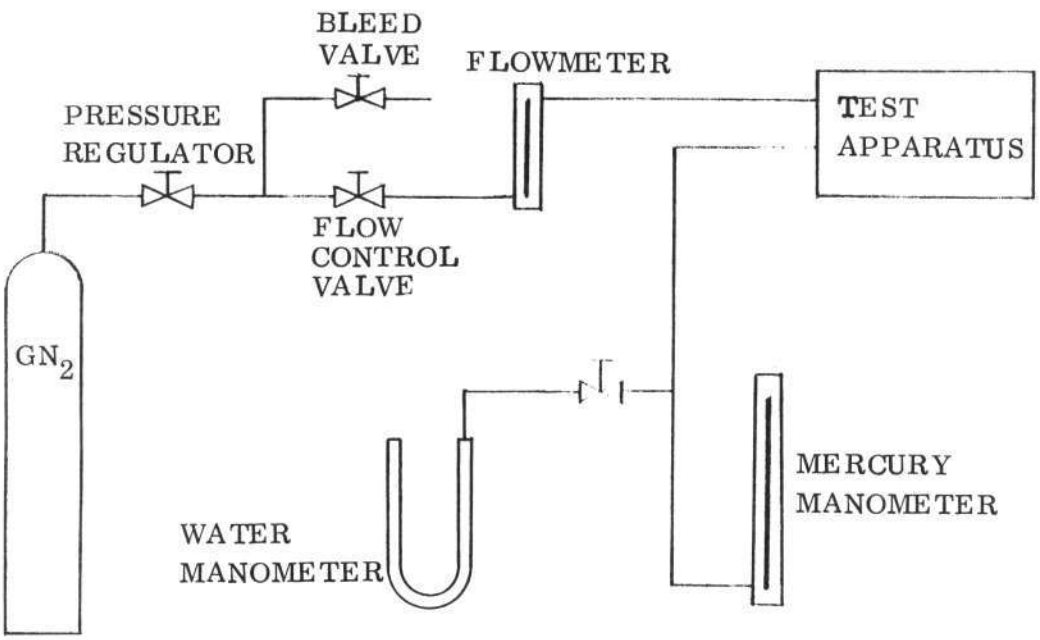


Figure 3-6: Schematic of Gas Flow Resistance Test Setup

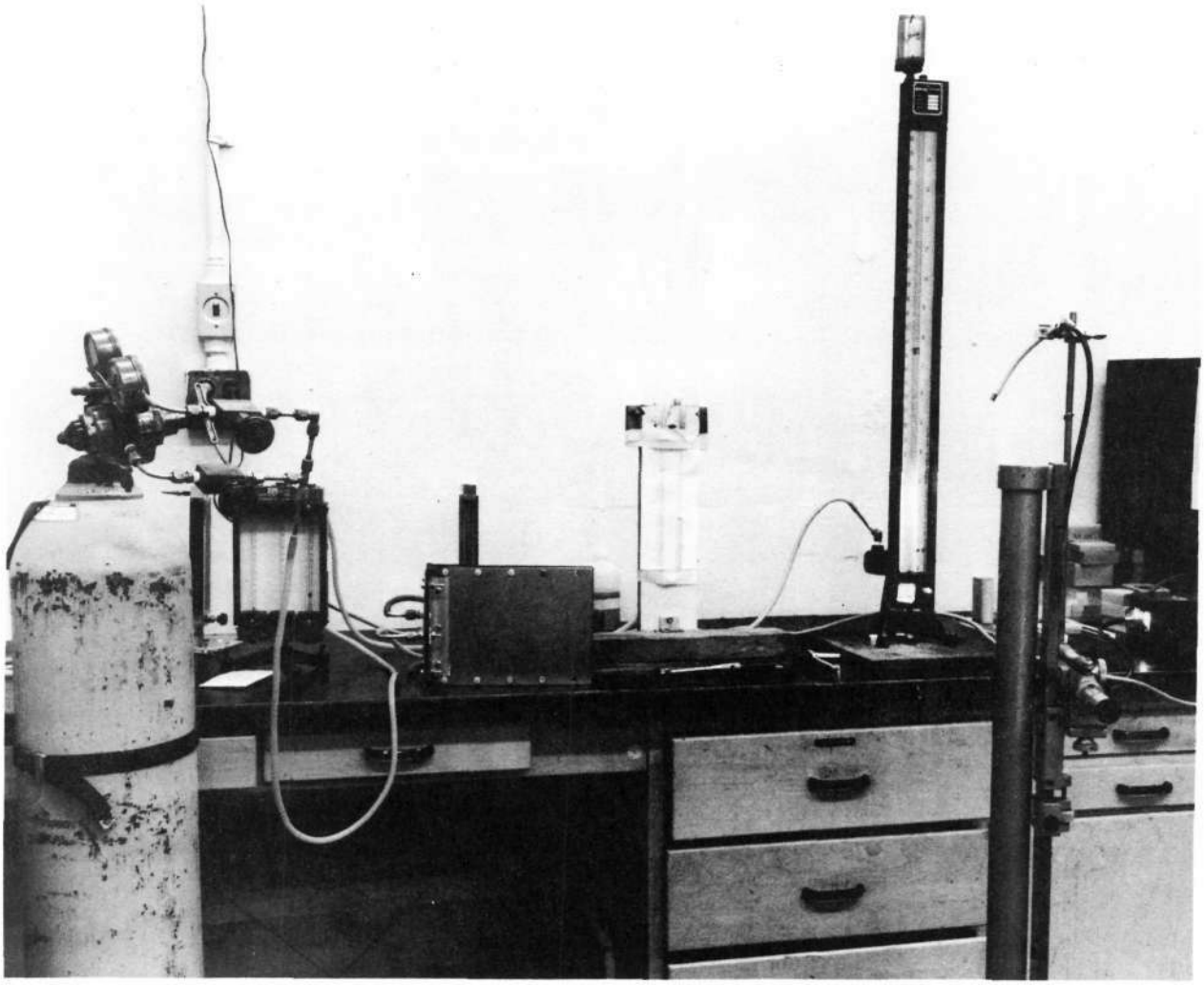

Figure 3-7. Gas Flow Resistance Test Setup

water and mercury manometers allow measurements to be taken over a very wide range of flow rates and pressures. Manometer readings were sighted with a cathetometer. A photograph of the test setup is shown in Figure 3-7.

Parallel gas flow tests have been performed on eight of the 71- panels using the cylindrical test beaker and two specimens for each panel. The test results are shown in Figure 3-8. The large variance in the gas flow resistance of the specimens is indicative of large differences in the internal structure of the various panels. An indication of the dispersion within a panel is provided by Figure 3-9 where the test results for both specimens of panels 71-23, -30 and -33 are plotted.

In an attempt to obtain more consistent data, a new parallel flow apparatus was devised for testing specimens from the 72- panel master order. By using the square beaker apparatus, both parallel and perpendicular flow tests could be performed on the same foam specimen. Also, the two test specimens from each panel were taken from adjacent locations in order to minimize variation between specimens. The results of the gas flow resistance tests on the 72- panels are presented in Table 3-1.

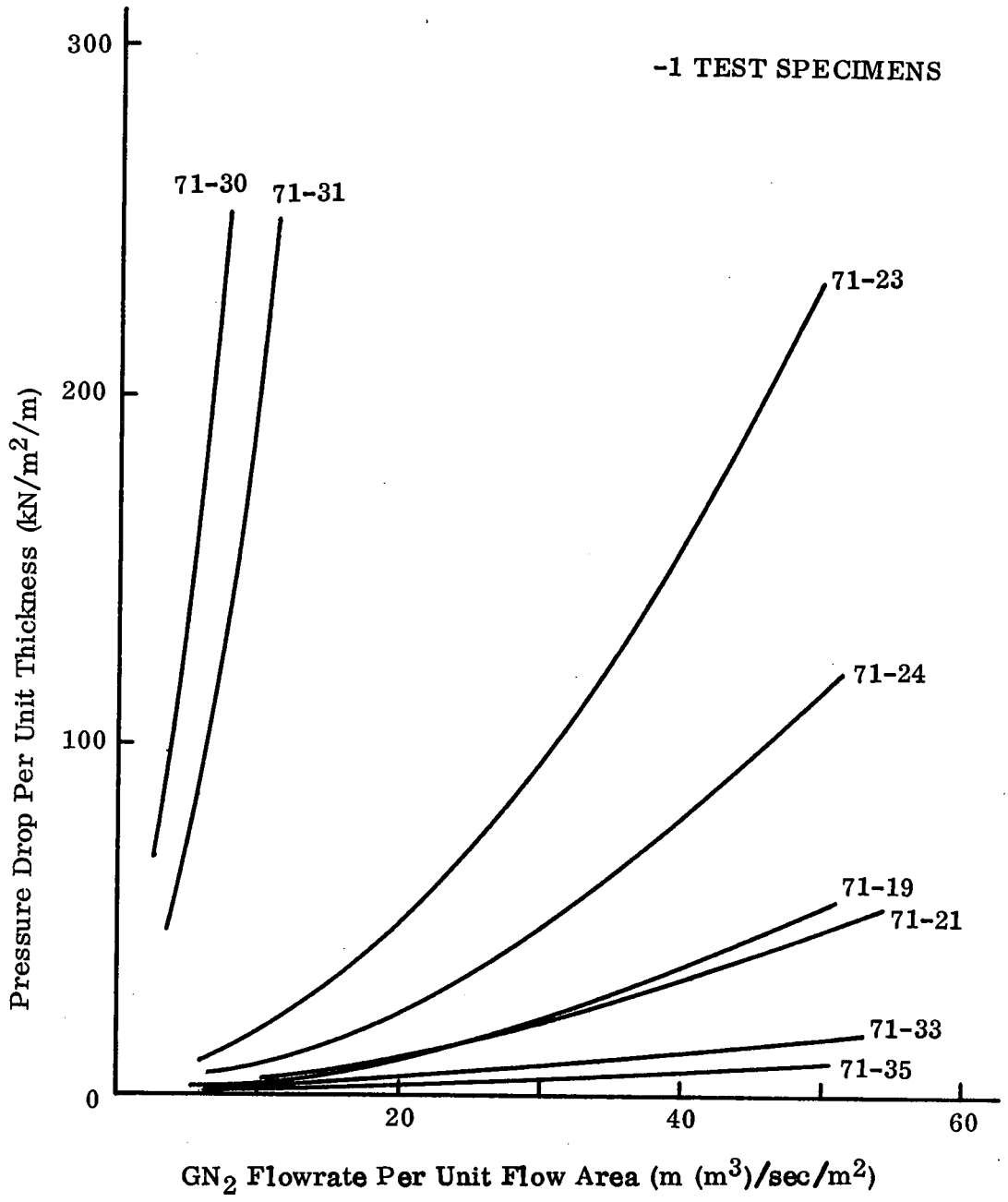


Figure 3-8. Parallel Gas Flow Test Results

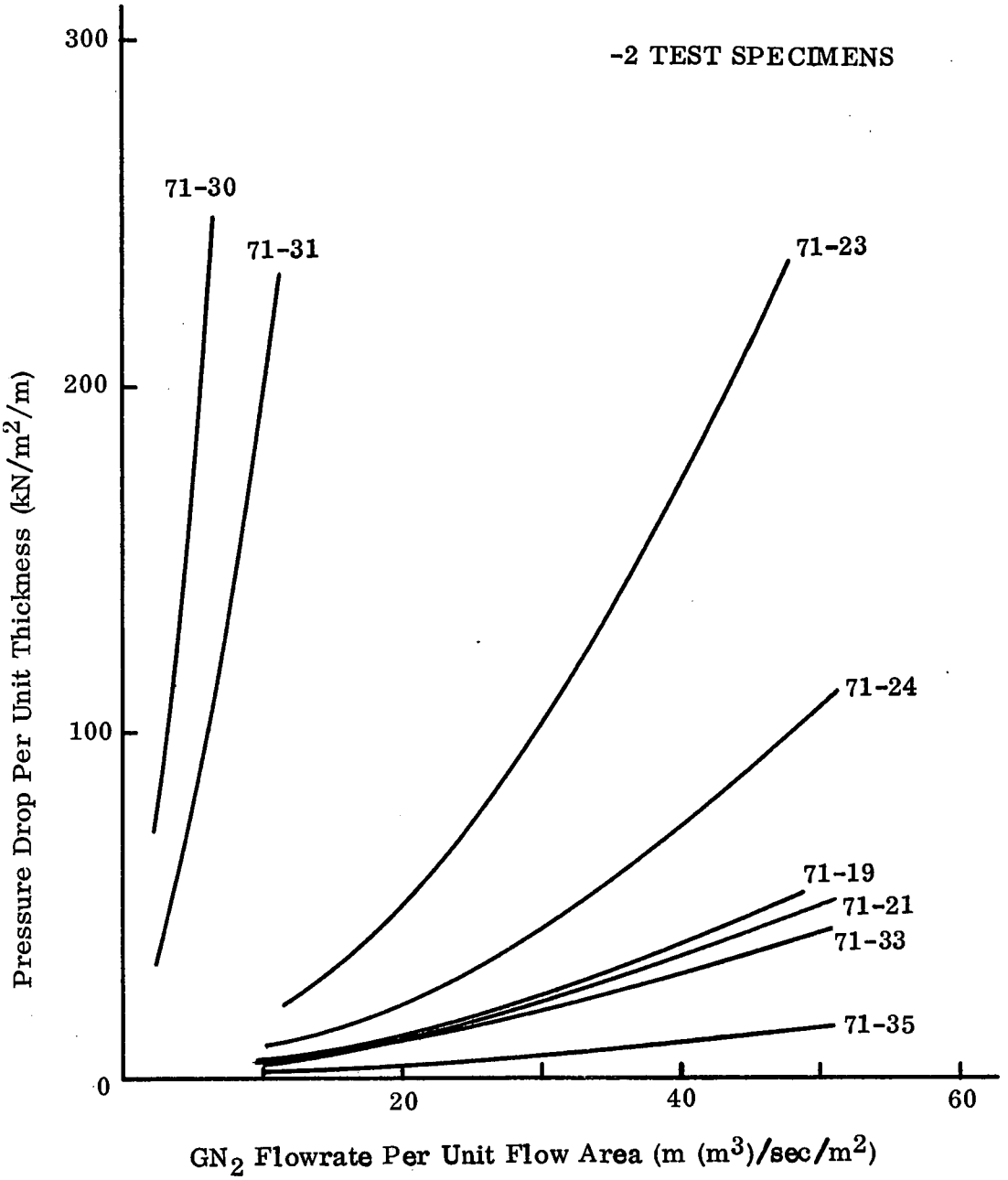


Figure 3-8. Concluded

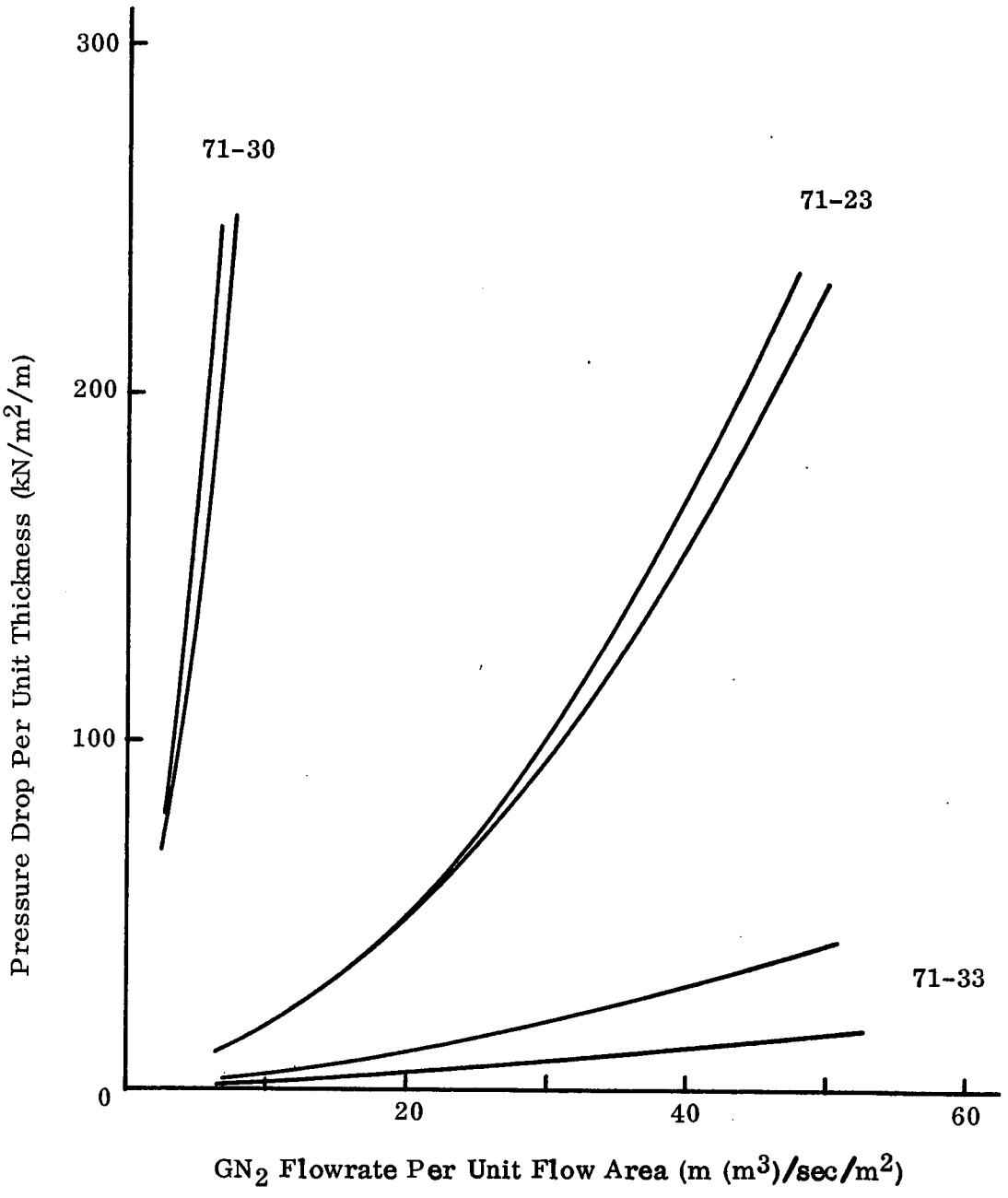


Figure 3-9. Comparison for Samples Cut from the Same Thermal Conductivity Specimen

Table 3-1. Gas Flow Resistance

| Panel | Gas Flow Resistance kN sec/m$^4$ (psi/in./SCFM $GN_2/ft^2$) Perpendicular | Parallel | Ratio | Thickness cm (in.) |
|---|---|---|---|---|
| 72-41 | 3911 (0.0732) | 1026 (0.0192) | 3.8 | 2.54 (1.0) |
| 72-74 | 6304 (0.118) | 581 (0.0109) | 10.8 | 2.54 (1.0) |
| 72-1 | 4381 (0.0820) | 1159 (0.0217) | 3.8 | 2.54 (1.0) |
| 72-18 | 1143 (0.0214) | 310 (0.00580) | 36.9 | 2.54 (1.0) |
| 72-55 | 930 (0.0174) | 104 (0.00195) | 8.9 | 2.54 (1.0) |
| 72-60 | 3489 (0.0653) | 641 (0.0120) | 5.4 | 2.54 (1.0) |
| 72-32 | 818 (0.0153) | 153 (0.00286) | 5.4 | 1.50 (0.59) |
| 72-29 | 5744 (0.108) | 784 (0.0147) | 7.3 | 4.60 (1.81) |
| 72-3 | 4291 (0.0803) | 1490 (0.0279) | 2.9 | 7.16 (2.82) |
| 72-34 | 449900 (8.42) | 212 (0.00397) | 2120 | 0.76 (0.30) |

All of the panels in Table 3-1 exhibit a low flow resistance in the direction parallel to the foam cells. In the perpendicular direction, the panels with a uniform appearance, panels 72-1, 34, 41 and 74, have a high flow resistance. Panel 72-60 has a severely curved cell structure and panels 72-18 and 55 have a low density center layer. The 2.54 cm (1.0 in.) panels cut from the surface of a 7.62 cm (3.0 in.) panel, such as panels 72-1, 41 and 74, have a more uniform appearance and better flow resistance than panels formed to their full thickness, such as panels 72-18, 55 and 60. Panel 72-34 was cut from the edge of a 7.62 cm (3.0 in.) panel, but it is only 0.76 cm (0.30 in.) thick. A comparison of the gas flow resistance data with the bulk density variations reveals no discernable correlation. Although no relation between thermal conductivity and parallel flow resistance could be found, panels with a high perpendicular flow resistance generally have a better thermal performance (see Section 4).

Figure 3-10 illustrates the variation of gas flow resistance within a panel. Panels were sliced into sheets and then tested for permeability perpendicular to the foam cells. From Figure 3-10, it is seen that the center layer in a panel accounts for the low perpendicular gas flow resistance of the foam. This correlates exactly with the density variations in a panel (see Section 5) where the center layer of a panel is less dense than the outer layers.

An extensive investigation of the cell structure of PPO foam has been carried out using the bubble point technique (Reference 3). Bubble point tests were used to evaluate cell size and shape by bubbling pressurant gas through the foam at measured temperatures and pressures. The conclusion of these tests was that the diameter of the foam cells must be greater in the interior of the foam than at the surface. Microscopic inspection of the foam and the results of gas flow resistance tests and density variation measurements (see Section 5) verify this conclusion.

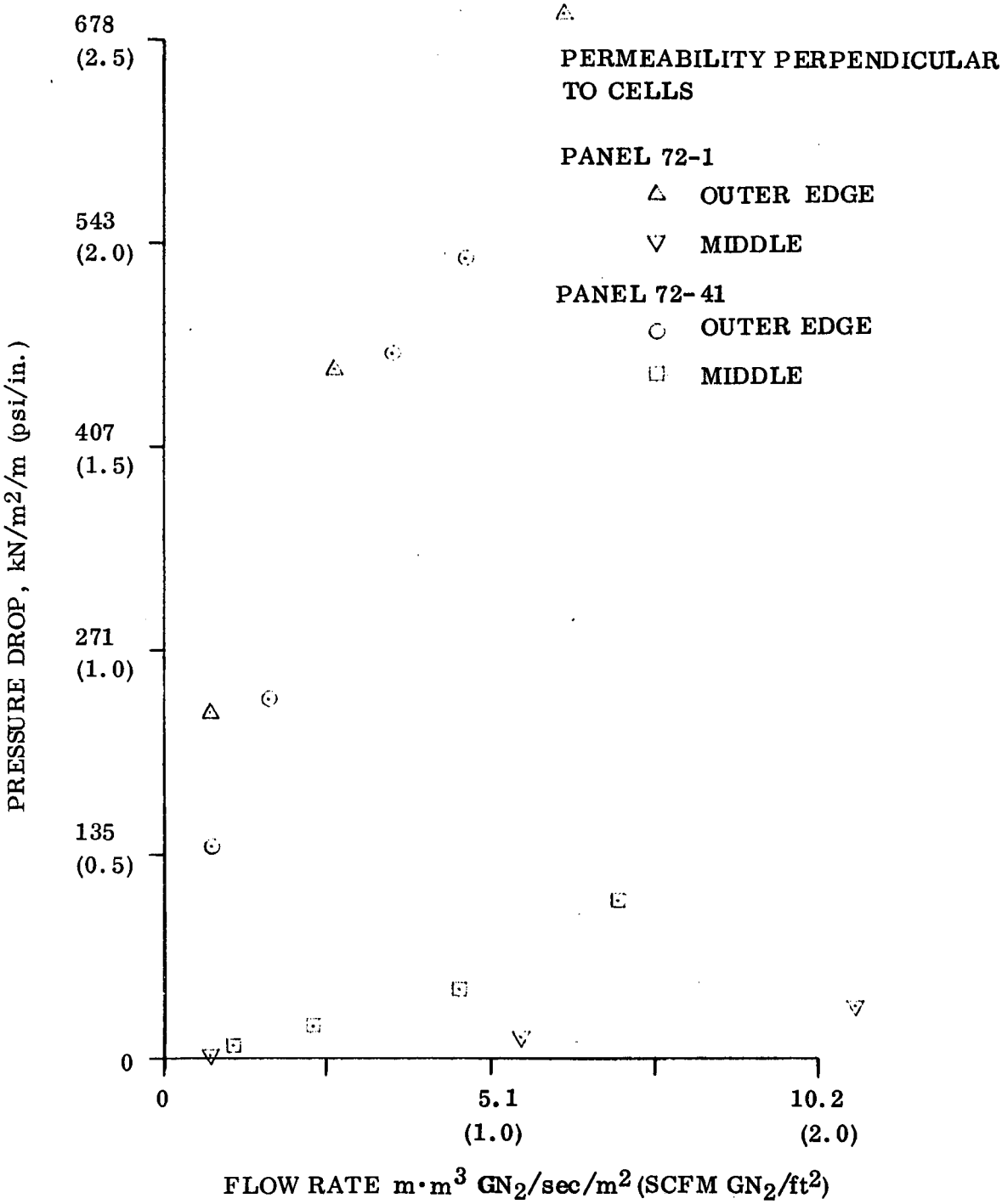


Figure 3-10. Variation of PPO Foam Permeability

## SECTION 4

## FLUID-THERMAL CORRELATION (1.2.3.2)

Results of the thermal conductivity tests have been compared with the results of the density gradient investigation, x-ray inspection and pressure drop tests to determine if any of these techniques could be employed to screen incoming panels before using them in an insulation system. Pressure drop tests and density gradient measurement are destructive test techniques while x-ray inspection has the advantage of being non-destructive.

Ten panels of the 72- panel master order were tested for thermal conductivity. Six of the ten were 25.4 mm (1.00 in) thick and can be compared among themselves. The other four panels tested ranged in thickness from 7.6 mm (0.30 in) to 71.6 mm (2.82 in). The first three panels listed in Table 4-1 were cut from the surface of 75 mm (2.95 in) panels while the last three were originally formed as 25.4 mm (1.0 in) panels. The thermal performance ranking of the six 25.4 mm (1.00 in) panels is given in Table 4-1.

Table 4-1. Thermal Performance Ranking, Composite (Vertical and Horizontal Orientations) Conductivity

| Panel | Rank | Relative Conductivity Ratio |
|---|---|---|
| 72-41 | 1 | 1.000 |
| 72-74 | 2 | 1.038 |
| 72-1 | 3 | 1.086 |
| 72-56 | 4 | 1.077 |
| 72-64 | 5 | 1.104 |
| 72-17 | 6 | 1.710 |

The x-ray inspection of the panels is most convenient in that it is non-destructive and can be performed as the panels are received before any machining is started. Sectioning panels after x-raying revealed that sometimes large voids are not evident in the x-rays. Also, undesirable cell curvature and low density center layers are not detectable by x-ray. Comparing x-rays of the panels in Table 4-1, the three highest ranked panels had a very uniform appearance. But, the sixth ranked panel also appeared quite uniform. Thus, if the x-ray reveals a defect, then the panel will likely have a poor thermal performance, but a panel with a uniform appearing x-ray might also have defects and a poor thermal performance.

Calculation of density variations throughout each panel and comparison with thermal performance reveals that panels with a more uniform density have a better thermal performance. Although there is no large difference in the uniformity of the three best thermal performance panels, Panel 72-41 had slightly smaller density variations

than Panels 72-74 and 72-1, which were about equal in uniformity. Panels formed to their final thickness, such as Panels 72-56, -64 and -17 (the three poorest thermal performance panels), have significantly greater density variations than panels cut from the surface of a thick panel (Panels 72-41, -74 and -1). Thus, thermal performance is moderately sensitive to the degree of density variation.

Resistance to gas flow both perpendicular and parallel to the foam cells was measured. Ideally, the flow resistance should be infinite perpendicular to the cells (to prevent lateral convection) and near zero parallel to the cells. The results of the gas flow tests are listed in Table 4-2. Panels 72-18, -55 and -60 are similar to Panels 72-17,

Table 4-2. Gas Flow Resistance

| Panel | Gas Flow Resistance kN sec/$m^4$ (psi/in./SCFM $GN_2/ft^2$) Perpendicular | Parallel | Ratio |
|---|---|---|---|
| 72-41 | 3911 (0.0732) | 1026 (0.0192) | 3.8 |
| 72-74 | 6304 (0.118) | 581 (0.0109) | 10.8 |
| 72-1 | 4381 (0.0820) | 1159 (0.0217) | 3.8 |
| 72-18 | 1143 (0.0214) | 310 (0.00580) | 36.9 |
| 72-55 | 930 (0.0174) | 104 (0.00195) | 8.9 |
| 72-60 | 3489 (0.0653) | 641 (0.0120) | 5.4 |

-56, and -64 (Table 4-1) in that they were originally formed as 25.4 mm (1.0 in.) panels. As seen from Table 4-2, the higher thermal performance panels have a higher gas flow resistance perpendicular to the cells. The low gas flow resistance in both directions of Panels 72-18, -55 and -60 is due to the low density center section of panels formed to their full final thickness. Such full thickness panels typically have a poor thermal performance, probably due to lateral convection through the porous midsection. Thus, high resistance to gas flow perpendicular to the foam cells is more important than low resistance parallel to the cells for good thermal performance.

Of the three techniques for predicting a panel's thermal performance, sectioning a panel for inspection and density gradient analysis is the best. A density gradient analysis will define porous regions, the same result obtained with the more difficult and time consuming gas flow resistance tests, and reveal defects not seen in x-rays. The x-ray technique is good in that it can be performed on all panels, but it has not been developed to the point where it can be relied upon to detect all panel defects.

## SECTION 5

## MATERIAL TESTING (1.1.2.3.3)

In the process of developing a better PPO foam, Convair Aerospace is evaluating density gradients for all new configurations received. This is being done to insure that a material with uniform thermo-physical properties is being developed.

Prior to cutting density gradient specimens from a panel, the initial steps are to remove the paper and trim the sides to make a rectangular panel. The panel is then weighed and measured; these values being used to compute a nominal density. Next, the panel is cut into thirds (t/3) and each piece is weighed and measured. These three sheets are then cut and labeled in accordance with Figure 5-1 for the smaller panels, and Figure 5-2 for the larger panels. Each piece is weighed and measured and the density computed. This density is then compared to the nominal density of the full panel.

The standard blowing agent for PPO foam panels has been dichloroethane (DCE). In April 1971, a panel, 71-11, was received which utilized a 3:1 parts by volume mixture of Chlorothene Nu (CNU) (1, 1, 1 trichloroethane) and dichloroethane (DCE) as the blowing agent. This panel, 43 × 33 × 5 cm (17 × 13 × 2 in.) with a nominal density of 33 kg/m$^3$ (2.06 pcf), has been tested to determine the extent of both longitudinal (parallel to the fiber orientation) and lateral density variations. The results of the investigation are summarized below.

| | |
|---|---|
| Measured nominal panel density | 33.0 kg/m$^2$ |
| Maximum longitudinal density variation from nominal | -6 percent |
| Maximum lateral density variation from nominal | 3 percent |
| Maximum density variation of any piece from nominal | -11 percent |

The density variations from the nominal value, 33.0 kg/m$^3$ (2.06 pcf), are shown in Figure 5-3. Note that the variations for the middle sheets are all lower than the nominal value while the variations for the outer sheets are generally higher. The largest single variation from nominal is -11 percent. By combining the pieces as shown in Figure 5-4 and averaging the densities of the combined pieces, the maximum lateral variation from the nominal density was found to be 3 percent.

After the 27 pieces had been cut from the panel, it was noticed that small flecks of solid material occurred throughout the foam. These flecks, shown in Figure 5-5, are apparently pockets of resin that failed to expand during the blowing process most likely due to incomplete mixing of the components. This information was transmitted to the

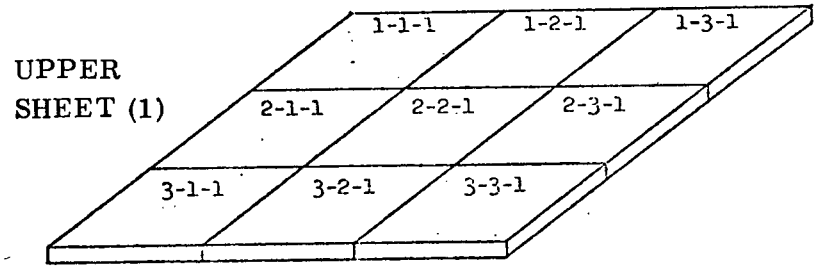


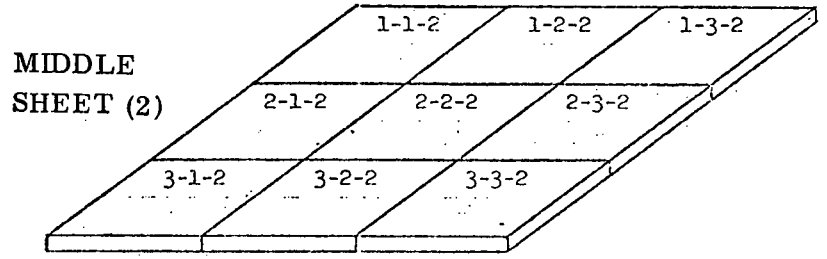


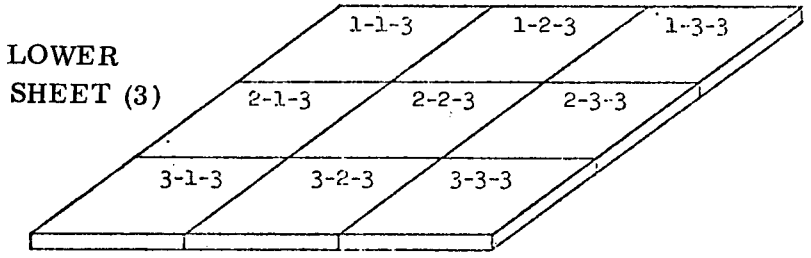


Figure 5-1. Identification of Cut Specimens (Small Panels)

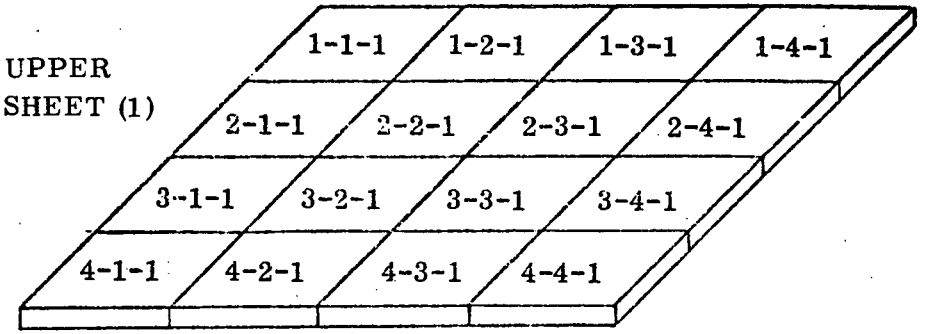


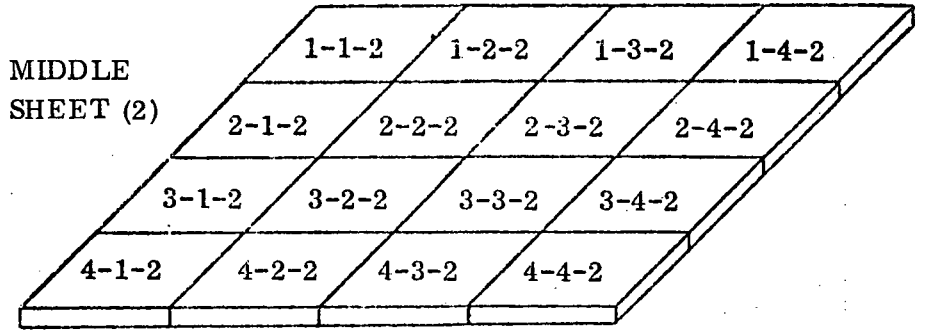


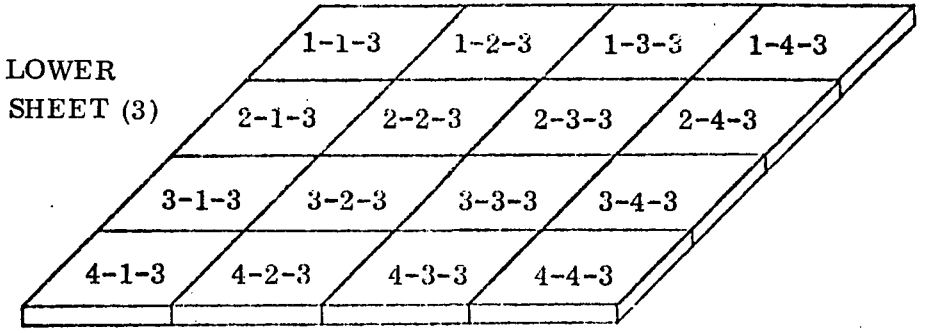


Figure 5-2. Identification of Cut Specimens (Large Panels)

NOMINAL DENSITY ($\rho_N$)

= 33.0 kg/m$^3$ (2.06 pcf)

VARIATION

$$= \frac{\rho - \rho_N}{\rho_N} \times 100\%$$

UPPER SHEET

| | | |
|---|---|---|
| -2 | 1 | 3 |
| -1 | 1 | 4 |
| 1 | 2 | 3 |

MIDDLE SHEET

| | | |
|---|---|---|
| -11 | -8 | -8 |
| -10 | -5 | -4 |
| -8 | -8 | -5 |

LOWER SHEET

| | | |
|---|---|---|
| 2 | 4 | 6 |
| 5 | 6 | 10 |
| 6 | 5 | 7 |

**Figure 5-3. Density Variations from Nominal, Panel 71-11**

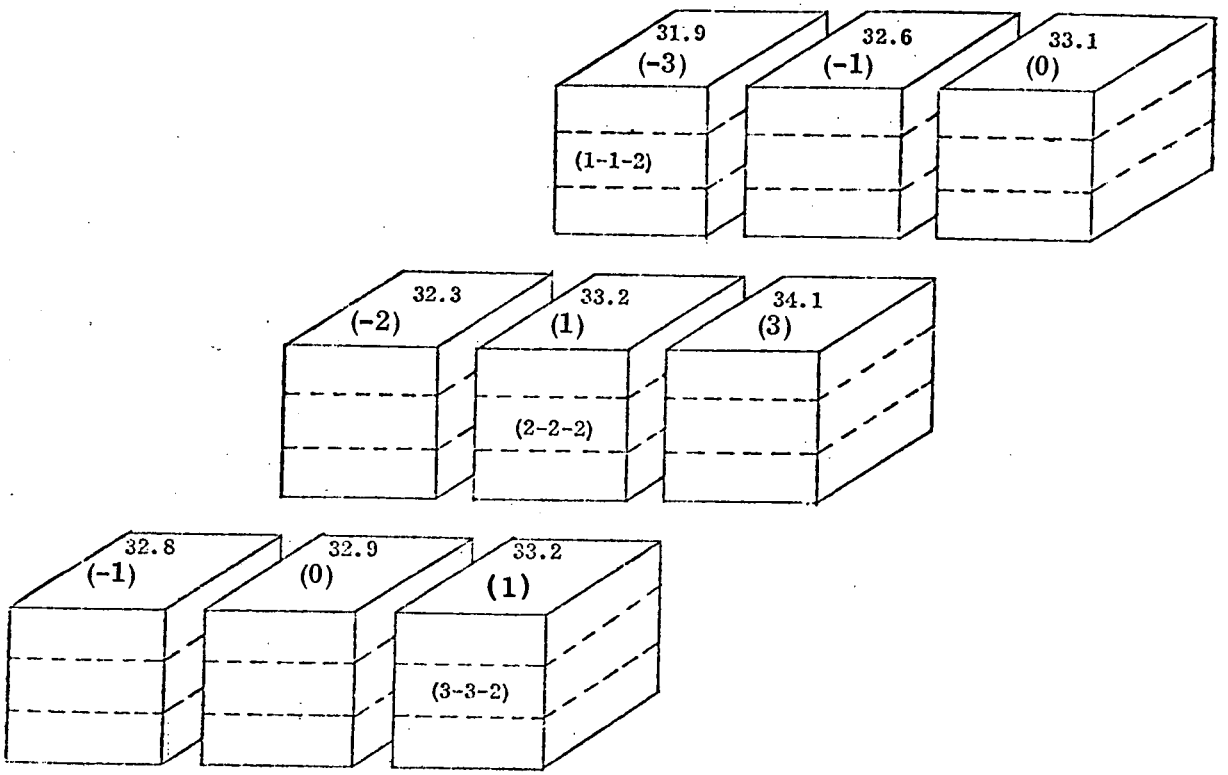


DENSITY IN KG/M$^3$
VARIATION IN PERCENT FROM NOMINAL (33.0 KG/M$^3$)

Figure 5-4. Average Density of Three-Piece Stacks and Percent Variation From Nominal

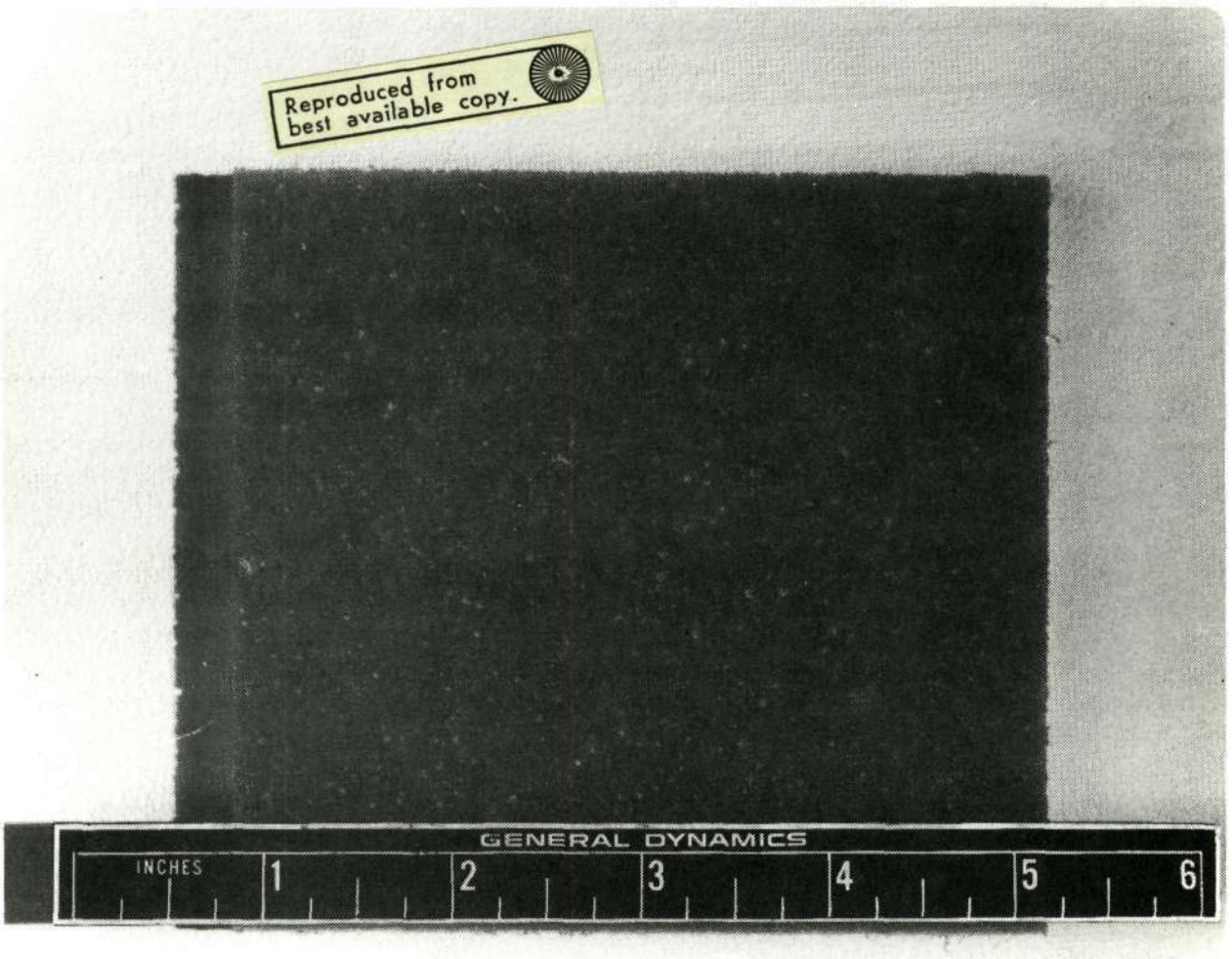


Figure 5-5. Solid Inclusion in the Foam Matrix

vendor and efforts have been made to alleviate the problem. The existence of the flecks has no apparent detrimental effect on the thermal or mechanical properties of the foam.

Two additional panels blown with DCE/CNU, panels 71-12 and -14, were also evaluated. The as-received densities of these panels were 30.4 and 28.8 kg/m$^3$ (1.9 and 1.9 pcf), respectively. Both panels were cut and labeled in accordance with Figure 5-1. The surfaces of Panel 71-14 were left in the as received condition whereas approximately 2.54 mm (0.1 inch) was removed with a bandsaw from both surfaces of Panel 71-12. Before any of the test pieces were cut from the panels, the panels were measured and weighed. Panel 71-12 had a nominal density of 30.1 kg/m$^3$ (1.88 pcf) and Panel 71-14 had a nominal density of 28.8 kg/m$^3$ (1.8 pcf). The densities of the individual pieces were computed along with the percent variation from the nominal and are illustrated in Figures 5-6 and 5-7. In general, the core of the panels had a lower density than the surface. The mean density of the middle sheet, Panel 71-14, was 24.5 kg/m$^3$ (1.53 pcf) while the upper and lower sheet had a combined mean density of 32.2 kg/m$^3$

PANEL 71-12

Density in pcf
(Variation)

UPPER SHEET
(1)

| | | |
|---|---|---|
| 1.988 (+6) | 2.080 (+11) | 1.998 (+6) |
| 2.027 (+8) | 2.140 (+14) | 1.985 (+5) |
| 1.933 (+3) | 2.042 (+9) | 1.970 (+5) |

Mean $\rho$ = 2.018 pcf (+7)

Nominal Density = 1.882 pcf

$$\text{Variation} = \frac{\rho - \rho_N}{\rho_N} \times 100\%$$

MIDDLE SHEET
(2)

| | | |
|---|---|---|
| 1.683 (-11) | 1.765 (-6) | 1.683 (-11) |
| 1.673 (-11) | 1.754 (-7) | 1.665 (-12) |
| 1.624 (-14) | 1.698 (-10) | 1.647 (-12) |

Mean $\rho$ = 1.688 pcf (-10)

LOWER SHEET
(3)

| | | |
|---|---|---|
| 2.097 (+11) | 2.159 (+15) | 2.090 (+11) |
| 2.166 (+15) | 2.230 (+18) | 2.081 (+11) |
| 2.062 (+10) | 2.100 (+12) | 2.009 (+7) |

Mean $\rho$ = 2.110 pcf (+12)

Figure 5-6. Densities of Individual Pieces and Percent Variation From Nominal, Panel 71-12

PANEL 71-14

Density in pcf
(Variation)

UPPER SHEET
(1)

| | | |
|---|---|---|
| 1.91 (+6) | 1.89 (+5) | 1.97 (+9) |
| 1.89 (+5) | 1.99 (+11) | 2.07 (+15) |
| 1.81 (+1) | 2.0 (+11) | 2.06 (+14) |

Mean $\rho$ = 1.954 pcf (+9)

Nominal Density = 1.8 pcf

Variation: $\frac{\rho - \rho_N}{\rho_N} \times 100\%$

MIDDLE SHEET
(2)

| | | |
|---|---|---|
| 1.45 (-19) | 1.41 (-22) | 1.47 (-18) |
| 1.58 (-12) | 1.58 (-12) | 1.65 (-8) |
| 1.45 (-19) | 1.54 (-14) | 1.63 (-9) |

Mean $\rho$ = 1.53 pcf (-15)

LOWER SHEET
(3)

| | | |
|---|---|---|
| 1.91 (9+) | 2.08 (+16) | 2.0 (+11) |
| 2.02 (+12) | 2.18 (+21) | 2.14 (+19) |
| 1.97 (+9) | 2.18 (+21) | 2.12 (+18) |

Mean $\rho$ = 2.07 pcf (+15)

Figure 5-7. Densities of Individual Specimens and Percent Variation from Nominal, Panel 71-14

(2.01 pcf). The largest variation from the nominal was -22% and was found in Panel 71-14, piece 1-2-2. The lateral density gradients are not quite as severe with the largest variation from the nominal being +9% and found in Panel 71-14, stack 2-3-X (Table 5-1).

Table 5-1. Maximum Deviations

| Panel | Overall Density $kg/m^3$ (pcf) | Max. Longitud. Density Variation From Nominal | Max. Lateral Density Variation From Nominal | Max. Density Variation of any Piece From Nominal |
|---|---|---|---|---|
| 71-12 | 30.1 (1.88) | 12% | +8% | +19% |
| 71-14 | 28.8 (1.80) | ±15% | +9% | -22% |

Density gradient tests were performed on eight of twelve panels received in August 1971. The data indicates that the four corners of all the panels are low density as compared to the nominal density. The core of the panels also has a lower density. Data from the eight panels is summarized in Table 5-2. The largest single piece variation from the nominal was 31% and occurred in Panel 71-18, piece 2-1-1. Overall, Panel 71-16 had the smallest density gradients while Panel 71-20 ranked second best.

Since the edge pieces from all eight panels had very large density variations, an analysis was made on only the twelve interior pieces from each panel and the nominal density was computed as the average density of the twelve pieces for each panel. The results of this analysis are given in Table 5-3. In all cases the nominal density of the twelve middle pieces is higher than the nominal density of the full panel.

Figure 5-8 is a photograph of the pieces which comprise the upper and middle sheets of Panel 71-22. The light area on piece 4-1-1 is cells which are oriented 0.787 rad (45°) with respect to the surface of the piece. Note the streaked appearance of the foam. The cell orientation takes on a curved pattern near the edges of the panel. This is shown in Figure 5-9 by separating the panel pieces.

Six additional 71- panels were cut into small pieces and the density of each calculated to determine the magnitude of longitudinal and lateral density variations through the panels.

Table 5-2. Density Gradient Summary Sheet

| Panel No. | Nominal Density | SHEET | | | | | | MAXIMUM VARIATION FROM NOMINAL FOR INDIVIDUAL PIECES | | | | | |
|---|---|---|---|---|---|---|---|---|---|---|---|---|---|
| | | UPPER | | MIDDLE | | LOWER | | From Upper Sheet | | From Middle Sheet | | From Lower Sheet | |
| | | ρ | % Var. From Nom. | ρ | % Var. From Nom. | ρ | % Var. From Nom. | Piece / ρ | % Var. From Nom. | Piece / ρ | % Var. From Nom. | Piece / ρ | % Var. From Nom. |
| 71-15 | 42.29 (2.64) | 47.74 (2.98) | 13 | 37.48 (2.34) | -11 | 46.77 (2.92) | 11 | 431 / 50.14 (3.13) | 19 | 142 / 35.56 (2.22) | -16 | 133 / 50.14 (3.13) | 19 |
| 71-16 | 38.60 (2.41) | 42.13 (2.63) | 9 | 35.24 (2.20) | -9 | 42.13 (2.63) | 9 | 421 / 45.33 (2.83) | 17 | 112 / 31.88 (1.99) | -17 | 323 / 45.65 (2.85) | 19 |
| 71-17 | 42.13 (2.63) | 47.09 (2.94) | 12 | 36.04 (2.25) | -15 | 49.18 (3.07) | 17 | 321 / 49.18 (3.07) | 17 | 442 / 32.52 (2.03) | -23 | 423 / 50.94 (3.18) | 21 |
| 71-18 | 42.77 (2.67) | 50.78 (3.17) | 19 | 40.85 (2.55) | -5 | 51.10 (3.19) | 19 | 211 / 56.07 (3.50) | 31 | 442 / 30.76 (1.92) | -27 | 313 / 51.74 (3.23) | 21 |
| 71-20 | 49.82 (3.11) | 53.02 (3.31) | 6 | 44.69 (2.79) | -10 | 55.74 (3.48) | 12 | 331 / 55.10 (3.44) | 11 | 442 / 40.85 (2.55) | -18 | 233 / 58.63 (3.66) | 18 |
| 71-22 | 45.17 (2.82) | 49.82 (3.11) | 10 | 39.41 (2.46) | -13 | 49.66 (3.10) | 10 | 331 / 51.58 (3.22) | 14 | 412 / 34.44 (2.15) | -24 | 343 / 50.78 (3.17) | 13 |
| 71-25 | 46.93 (2.93) | 51.58 (3.22) | 10 | 42.13 (2.63) | -10 | 55.74 (3.48) | 19 | 331 / 52.38 (3.27) | 12 | 142 / 39.41 (2.46) | -16 | 323 / 56.23 (3.57) | 20 |
| 71-26 | 47.90 (2.99) | 52.86 (3.30) | 10 | 44.05 (2.75) | -8 | 51.26 (3.20) | 7 | 231 / 54.62 (3.41) | 14 | 112 / 40.69 (2.54) | -15 | 233 / 53.02 (3.31) | 11 |

Table 5-3. Density Gradient Summary Sheet on Twelve Interior Pieces Only, Nominal Density Based on Twelve Pieces

| Panel No. | Nominal Density | SHEET | | | | | | MAXIMUM VARIATION FROM NOMINAL FOR INDIVIDUAL PIECES | | | | | |
|---|---|---|---|---|---|---|---|---|---|---|---|---|---|
| | | UPPER | | MIDDLE | | LOWER | | From Upper Sheet | | From Middle Sheet | | From Lower Sheet | |
| | | ρ | % Var. From Nom. | ρ | % Var. From Nom. | ρ | % Var. From Nom. | Piece / ρ | % Var. From Nom. | Piece / ρ | % Var. From Nom. | Piece / ρ | % Var. From Nom. |
| 71-15 | 45.01 (2.81) | 48.38 (3.02) | +7 | 39.25 (2.45) | -13 | 47.42 (2.96) | +5 | 321 / 49.02 (3.06) | 9 | 232 / 38.60 (2.41) | -14 | 223 / 47.74 (2.98) | 6 |
| 71-16 | 41.97 (2.62) | 43.73 (2.73) | +4 | 37.32 (2.33) | -11 | 44.85 (2.80) | +7 | 321 / 44.37 (2.77) | 6 | 222 / 36.84 (2.30) | -12 | 323 / 45.65 (2.85) | 9 |
| 71-17 | 45.65 (2.85) | 48.38 (3.02) | +6 | 37.30 (2.36) | -17 | 50.46 (3.15) | +11 | 321 / 49.18 (3.07) | 8 | 332 / 37.32 (2.33) | -18 | 233 / 50.94 (3.18) | 12 |
| 71-18 | 45.97 (2.87) | 51.26 (3.20) | +12 | 38.12 (2.38) | -17 | 48.38 (3.02 | +5 | 221 / 42.22 (3.26) | 14 | 332 / 37.64 (2.35) | -18 | 223 / 49.18 (3.07) | 7 |
| 71-20 | 53.50 (3.34) | 54.46 (3.40) | +2 | 47.42 (2.96) | -11 | 58.15 (3.63) | +9 | 331 / 55.10 (3.44) | 3 | 332 / 46.93 (2.93) | -12 | 233 333 / 58.63 (3.66) | 10 |
| 71-22 | 47.42 (2.96) | 50.78 (3.17) | +7 | 38.44 (2.40) | -19 | 49.82 (3.11) | +5 | 331 / 51.58 (3.22) | 9 | 332 / 41.33 (2.58) | -13 | 323 / 50.46 (3.15) | 6 |
| 71-25 | 50.14 (3.13) | 51.90 (3.24) | +4 | 42.93 (2.65) | -14 | 55.74 (3.48) | +11 | 331 / 52.38 (3.27) | 4 | 332 / 42.13 (2.63) | -16 | 323 / 56.23 (3.51) | 12 |
| 71-26 | 50.78 (3.17) | 54.30 (3.39) | +7 | 45.33 (2.83) | -11 | 52.54 (3.28) | +3 | 231 / 54.62 (3.41) | 8 | 232 / 45.01 (2.81) | -11 | 233 333 / 53.02 (3.31) | 4 |

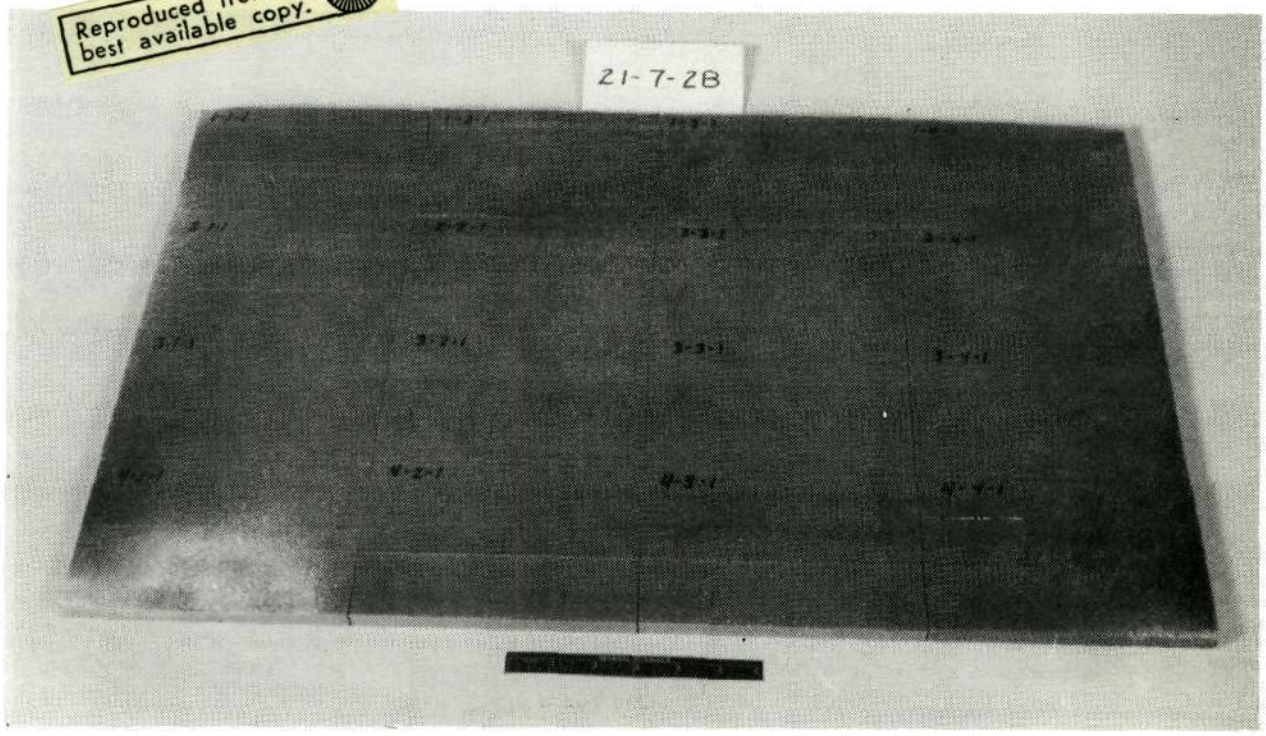


Figure 5-8a. Panel 71-22 Density Gradient Specimens, Upper Sheet

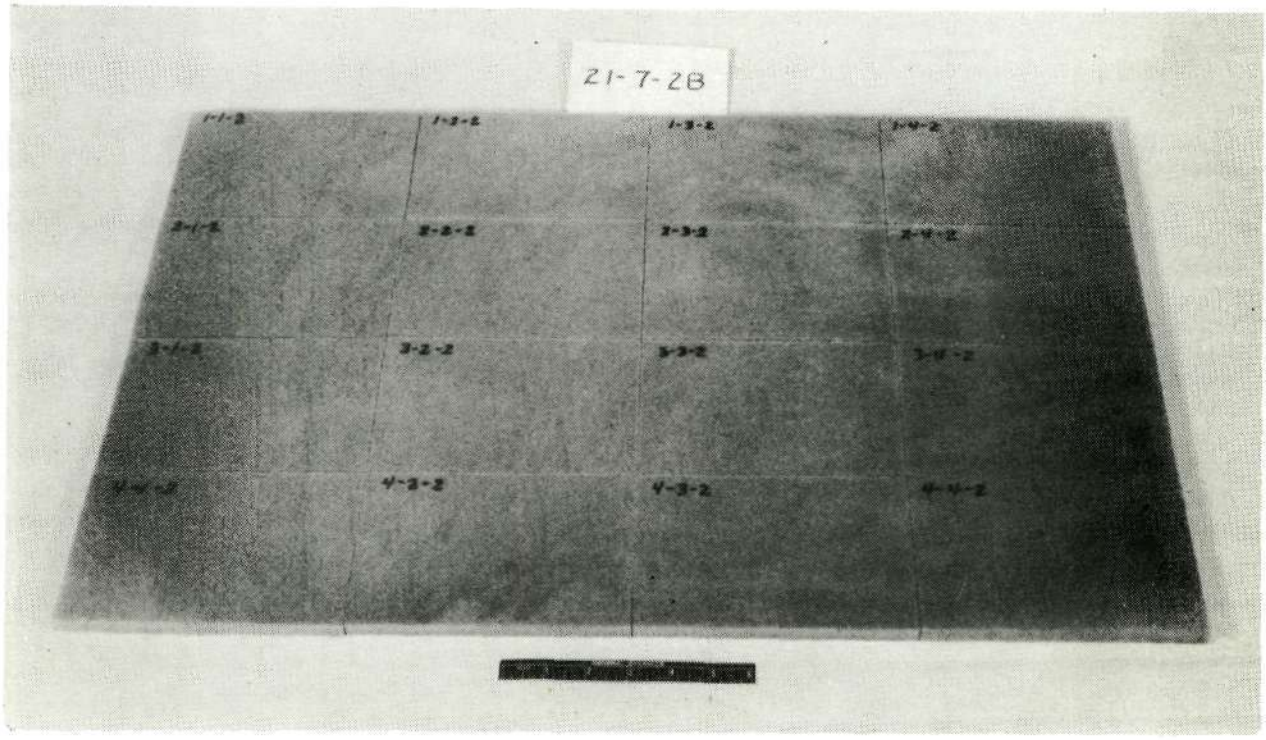


Figure 5-8b. Panel 71-22 Density Gradient Specimens, Middle Sheet

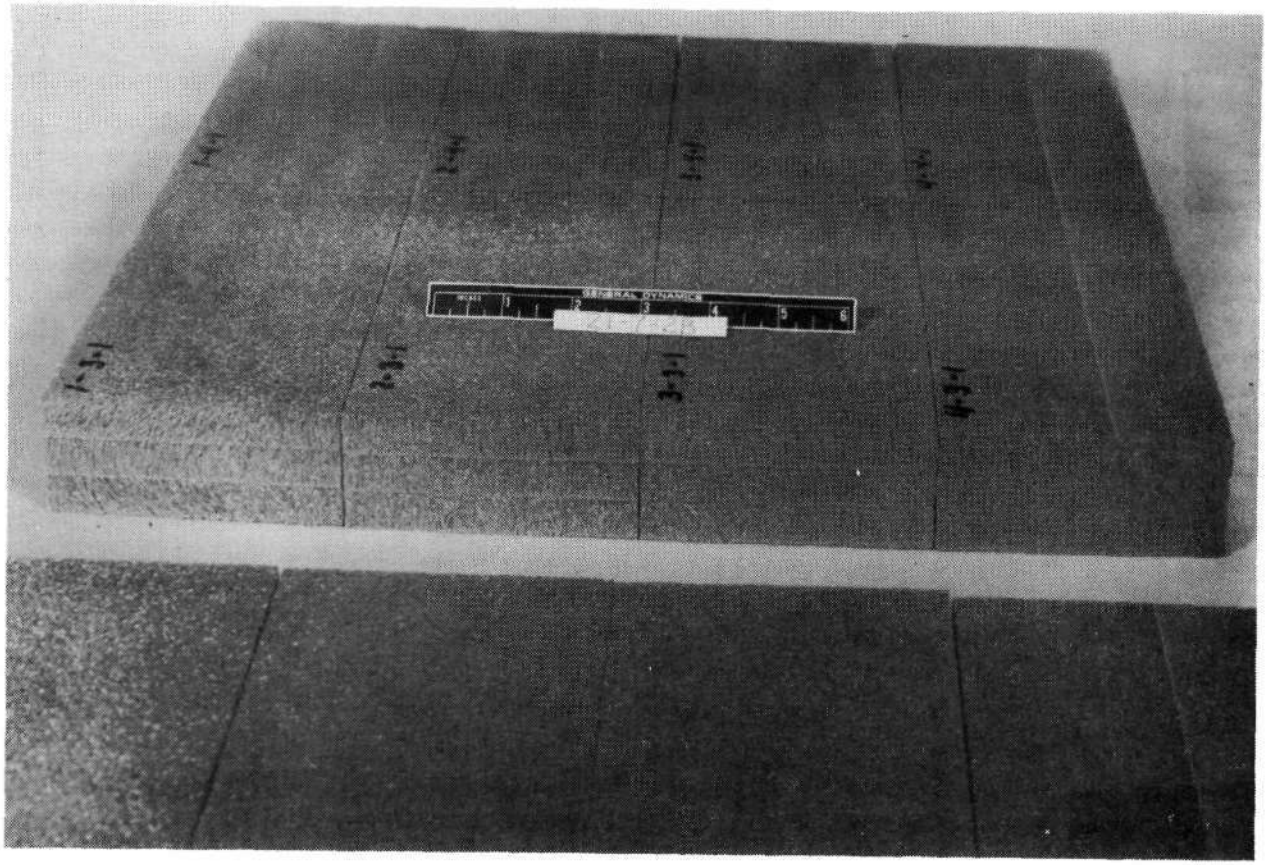

Figure 5-9. Panel 71-22 Irregular Cell Pattern

Initially each panel was sliced into three sheets corresponding to the upper, middle, and lower thirds of the panel. These sheets were weighed and measured and the densities were calculated. These data provided a measurement of the average variation between the middle and outer thirds and the variation of the density of each sheet from the measured ("nominal") density of the whole panel, taken after the paper had been removed and the edges squared. Finally, each sheet was cut into 16 equal pieces, each of which was weighed and measured. The densities of these pieces were then compared with each other and with the nominal panel density.

Due to the manner in which the foam is blown, the material in the center of the panel (measured parallel to the cell orientation) is less dense than that near the edges and exhibits higher lateral permeability, i.e., lower resistance to the movement of gas in the direction perpendicular to the cell orientation. This reduced density and higher permeability results in a reduction of the mechanical strength of the foam and increased thermal conductivity due to instability of the gas layer caused by lateral gas movement. Ideally there should be no density gradients in a panel and the lateral permeability should be constant across the cross section. Then the bulk density of the panel could be adjusted such that the lateral permeability, which would then be proportional to the density, is maintained below a maximum allowable level.

A summary of the density data is presented in Table 5-4. The first four panels listed in Table 5-4 were all blown with the dichloroethane (DCE) and petroleum ether (SBP) blowing agents and the last two, Panels 71-34 and -36, were blown with only the DCE agent. The 71-36 panel was blown from an injection molded millsheet while the others were blown from rolled sheets. The nominal densities of the panels ranged from a low of 37.6 kg/$m^3$ (2.35 pcf) up to a high of 46.1 kg/$m^3$ (2.88 pcf). The variations in the densities of the three sheets from the nominal panel values ranged from a high of +14 percent on the outer sheets to a low of -15 percent on the inner sheets. In general, the sheets cut from the -34 and -36 panels showed larger variations from the nominal than did the sheets cut from the other four panels. A similar conclusion can be drawn from the data shown in Table 5-4 for the individual pieces. Both the largest positive and negative variations from the nominal values occur in pieces cut from Panels 71-34 and -36. Also, the two panels blown with DCE ranked sixth and eighth best out of the eight panels subjected to thermal performance testing. The panels blown with DCE are clearly inferior to the panels blown with the combination of DCE and SBP both in terms of uniformity of internal structure and overall thermal performance.

A total of 17 five-cm (two-inch) thick panels were sliced into sheets and then cut into small pieces for density variation analysis. Of these 17, 11 were manufactured with the DCE/CNU combination of blowing agents, four with the DCE/SBP combination, and two with the single DCE agent. In general the DCE/CNU panels exhibited the least average density variation from the nominal values, the DCE/SBP panels only slightly higher, and the two DCE panels exhibited considerably higher average density variations than the other panels tested. It should be noted that this same ranking applies to the thermal conductivity results where the DCE/CNU panels were clearly the best. The clear superiority of the DCE/CNU blowing agent combination with regard to uniformity and thermal performance was the primary factor resulting in its selection for use in the 72-panel master order.

Table 5-5 shows the variation in densities of the 72- panels in the as-received condition, without the paper being removed. The spread of individual panel densities about the nominal, or target value, increases with the nominal density. Nine 10.2 cm (4 in) by 10.2 cm (4 in) pieces were cut from each of ten panels of the 72-panel master order (Figure 5-10) for determination of density variations in the panels by weighing and measuring each piece. The densities of each of the nine pieces were first calculated to determine the lateral density variations across the panels. Then each of the nine pieces was cut horizontally into thirds in order to measure the longitudinal density variations through the panel thickness.

Table 5-6 summarizes the results of the density measurements made on each panel. The largest lateral density variation measured was -10%. The results of the measurements on the upper, middle and lower thirds of the panel reveals the magnitude of the longitudinal density variation. Comparing either the upper or lower sheet with the middle sheet (or the upper sheet with the lower sheet for panels cut from the edge of a thicker panel (suffix U), it is seen that the material in the center of the panels is of considerably lower density and the maximum variation between the one-third thickness

Table 5-4. Summary of Density Variations Within Panels

| Panel No. | Nominal Density | SHEET | | | | | | MAXIMUM VARIATION FROM NOMINAL FOR INDIVIDUAL PIECES | | | | | |
|---|---|---|---|---|---|---|---|---|---|---|---|---|---|
| | | UPPER | | MIDDLE | | LOWER | | From Upper Sheet | | From Middle Sheet | | From Lower Sheet | |
| | | ρ | % Var. From Nom. | ρ | % Var. From Nom. | ρ | % Var. From Nom. | Piece / ρ | % Var. From Nom. | Piece / ρ | % Var. From Nom. | Piece / ρ | % Var. From Nom. |
| 71-27 | 40.2 (2.51) | 42.8 (2.67) | 6 | 35.5 (2.22) | -12 | 43.9 (2.74) | 9 | 331 / 47.5 (2.97) | 19 | 112 / 34.3 (2.14) | -15 | 333 / 47.1 (2.94) | 17 |
| 71-28 | 38.9 (2.43) | 42.1 (2.63) | 8 | 33.8 (2.11) | -13 | 41.8 (2.61) | 8 | 121 / 46.1 (2.88) | 19 | 342 / 33.1 (2.07) | -15 | 123 / 44.5 (2.78) | 14 |
| 71-29 | 38.1 (2.38) | 42.1 (2.63) | 11 | 34.6 (2.16) | -9 | 41.6 (2.60) | 9 | 231 / 44.2 (2.76) | 16 | 312 / 33.0 (2.06) | -14 | 143 / 44.5 (2.78) | 17 |
| 71-32 | 45.8 (2.86) | 51.8 (3.24) | 13 | 40.7 (2.54) | -11 | 50.8 (3.17) | 11 | 231 / 54.8 (3.42) | 20 | 312 / 38.3 (2.39) | -17 | 123 / 52.5 (3.28) | 15 |
| 71-34 | 46.1 (2.88) | 51.6 (3.22) | 12 | 39.7 (2.48) | -14 | 51.7 (3.23) | 12 | 321 / 54.0 (3.37) | 17 | 132 / 37.0 (2.31) | -20 | 323 / 53.3 (3.33) | 16 |
| 71-36 | 37.6 (2.35) | 42.6 (2.66) | 13 | 32.0 (2.00) | -15 | 42.9 (2.68) | 14 | 331 / 44.0 (2.75) | 17 | 412 / 28.3 (1.77) | -25 | 233 / 45.0 (2.81) | 20 |

Table 5-5. Density Variations of Manufactured Panels

| Nominal Density ($kg/m^3$) | Panel Density ($kg/m^3$) | 72 - Panel Number | | |
|---|---|---|---|---|
| | | Thickness = 25 cm | Thickness = 50 cm | Thickness = 75 cm |
| 50 | 63 | 64 | | |
| 50 | 62 | | | |
| 50 | 61 | 66, 68 | | |
| 50 | 60 | 60, 61 | | |
| 50 | 59 | 67, 69 | | |
| 50 | 58 | 63, 65 | | |
| 50 | 57 | 59, 62, 70 | | 74 |
| 50 | 56 | | | |
| 50 | 55 | | | 71 |
| 50 | 54 | | | 73 |
| 50 | 53 | | | 72 |
| 50 | 52 | | | 76 |
| 50 | 51 | | | 75 |
| 40 | 46 | 48, 50, 53, 54, 55 | | |
| 40 | 45 | 52, 56 | 38 | 43 |
| 40 | 44 | 47, 51 | 32, 33, 39 | 45 |
| 40 | 43 | | | 42, 44 |
| 40 | 42 | 49, 57, 58 | 30,34, 35, 36, 37, 40 | 46 |
| 40 | 41 | | 29, 31 | |
| 40 | 40 | | | 41 |
| 30 | 33 | 7,8,9, 10, 11, 12, 13, 14, 15, 16, 17, 18 | | |
| 30 | 32 | | 23 | |
| 30 | 31 | | 24, 26, 27, 28 | |
| 30 | 30 | | | |
| 30 | 29 | | 25 | 1, 2, 3, 4, 5, 6 |

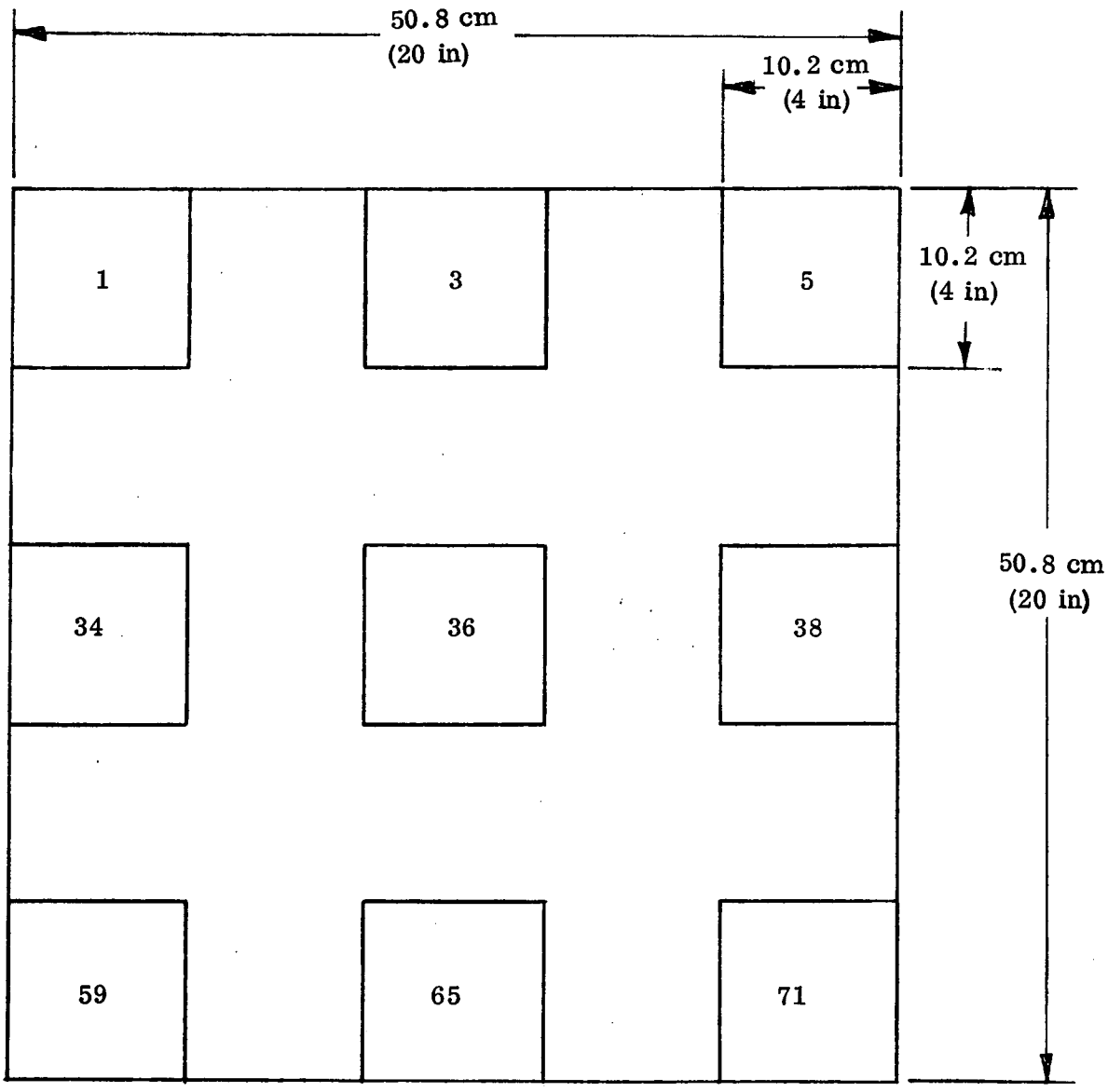


Figure 5-10. Identification of Cut Density Specimens for 72 - Panels

Table 5-6. Summary of Density Variations, 72 - Panels

| Panel No. | Original Thickness cm (in.) | Test Thickness cm (in.) | Nominal Density $kg/m^3$ ($lb/ft^3$) | Maximum Lateral Variation From Nominal % | Variation From Nominal % | | | Maximum Longitudinal Variation from Nominal % | | |
|---|---|---|---|---|---|---|---|---|---|---|
| | | | | | Upper Sheet | Middle Sheet | Lower Sheet | Upper Sheet | Middle Sheet | Lower Sheet |
| 72-1U | 7.62 (3) | 2.54 (1.00) | 28.49 (1.78) | -7 | +13 | +7 | -14 | +28 | +13 | -16 |
| 72-3 | 7.62 (3) | 7.14 (2.81) | 25.25 (1.58) | +5 | +13 | -26 | +12 | +19 | -32 | +18 |
| 72-18 | 2.54 (1) | 2.54 (1.00) | 28.11 (1.75) | +9 | +9 | -17 | +17 | +18 | -15 | +22 |
| 72-29 | 5.08 (2) | 4.60 (1.81) | 38.65 (2.41) | -6 | +6 | -10 | +6 | +6 | -12 | +4 |
| 72-32U | 5.08 (2) | 1.50 (.59) | 44.49 (2.78) | +5 | - | - | - | - | - | - |
| 72-34U | 5.08 (2) | .76 (.30) | 46.23 (2.89) | -5 | - | - | - | - | - | - |
| 72-41U | 7.62 (3) | 2.54 (1.00) | 40.92 (2.55) | -4 | +14 | +2 | -13 | +20 | +5 | -11 |
| 72-55 | 2.54 (1) | 2.51 (.99) | 40.94 (2.56) | -10 | +9 | -4 | +8 | +6 | -14 | +3 |
| 72-60 | 2.54 (1) | 2.45 (.98) | 50.07 (3.13) | -10 | +30 | -25 | -2 | +38 | -32 | -13 |
| 72-74U | 7.62 (3) | 2.45 (.98) | 61.19 (3.82) | -8 | 0 | +9 | -7 | -11 | +8 | -2 |

sheets of a panel is 55%. Panels 72-32U and 72-34U were too thin to cut into thirds. Looking at each of the nine pieces cut from each panel, the maximum longitudinal density variation is 70%.

The mechanical strength of PPO foam has been evaluated at temperatures of 21K (-423F), 294K (70F) and 423K (300F) for a wide range of foam densities. Strength tests were performed in the longitudinal (along the foam cells) and transverse (perpendicular to the foam cells) directions for both tension and compression. The results of the strength tests have been correlated with the density of the foam.

The strength tests were performed according to ASTM C297. For the longitudinal tests, 5.08 cm (2 in) square by t thick PPO foam blocks were used. The transverse specimens were 2.54 cm (1 in) high by 5.08 cm (2 in) long by t thick. In the compression tests, the foam blocks were placed between two parallel hardened steel platens. The tensile specimens were bonded to aluminum blocks which were then pinned into fixtures which were gimballed in two directions to insure that only axial loads were applied to the specimen. The specimens to be tested at 294K (70F) and 423K(300F) were bonded using Epon 934 epoxy adhesive while the specimens to be tested at 21K (-423F) were bonded using Crest 7343 polyurethane adhesive. All tensile failures occurred in the foam. The temperatures of the tests were controlled by two methods. The specimens tested at 21K(-423F) were submerged in liquid hydrogen. Each specimen was held in the $LH_2$ for five minutes before starting the test to allow it to come to equilibrium. The tests at 423K (300F) were run in a Missimers chamber. The specimen temperature was measured with a thermocouple and the specimens were held at 423K (300F) for ten minutes to allow them to come to equilibrium.

The results of the mechanical strength tests are summarized in Tables 5-7 through 5-10. Since the foam specimens do not fail in transverse compression, the tests were stopped at 20% deformation and the yield strength taken at a 2% offset. Typical stress failures are shown in Figures 5-11 through 5-13. Figure 5-11 shows the two locations where longitudinal compressive failures occurred. The compressive failures occur in the low density layer of the foam; which is the center region for panels formed to their final thickness (specimen on the right in Figure 5-11) and the lower surface for panels cut from the outer third of a large panel (specimen on the left in Figure 5-11). Figure 5-12 shows transverse (specimen on the left) and longitudinal (specimen on the right) tensile failures. Figure 5-13 compares a transverse tension specimen tested at 294K (70F) with a similar specimen from the same foam panel tested at 423K (300F). Note that the specimen run at 423K (300F) necked down while specimens run at the lower temperatures show no signs of necking down.

Table 5-7. Longitudinal Tensile Strength of PPO Foam

| Temp. \ Panel No. | Strength, $kN/m^2$ (psi) | | | | | | | | | |
|---|---|---|---|---|---|---|---|---|---|---|
| | 72-1U | | 72-3 | | 72-18 | | 72-29 | | 72-32U | |
| 21K (-423F) | 1655 | (240) | 1103 | (160) | 1772 | (257) | 1538 | (223) | 2089 | (303) |
| | 1427 | (207) | 876 | (127) | 1669 | (242) | 1710 | (248) | 1862 | (270) |
| | 1482 | (215) | 938 | (136) | 1358 | (197) | 1296 | (188) | 1696 | (246) |
| | 1517 | (220) | 972 | (141) | 1600 | (232) | 1517 | (220) | 1882 | (273) |
| Ambient | 1214 | (176) | 703 | (102) | 1827 | (265) | 1510 | (219) | 2158 | (313) |
| | 1151 | (167) | 841 | (122) | 1896 | (275) | 1524 | (221) | 2158 | (313) |
| | 1379 | (181) | 662 | (96) | 1937 | (281) | 1620 | (235) | 2151 | (312) |
| | 1248 | (175) | 731 | (106) | 1889 | (274) | 1551 | (225) | 2158 | (313) |
| 450K (+300F) | 615 | (89) | 365 | (53) | 952 | (138) | 745 | (108) | 972 | (141) |
| | 538 | (78) | 372 | (54) | 876 | (127) | 696 | (101) | 1048 | (152) |
| | 607 | (88) | 352 | (51) | 896 | (130) | 710 | (103) | 1034 | (150) |
| | 586 | (85) | 359 | (52) | 903 | (131) | 717 | (104) | 1020 | (148) |

| Temp. \ Panel No. | Strength, $kN/m^2$ (psi) | | | | | | | | | |
|---|---|---|---|---|---|---|---|---|---|---|
| | 72-34U | | 72-41U | | 72-55 | | 72-60 | | 72-74U | |
| 21K (-423F) | 2751 | (399) | 1669 | (242) | 1772 | (257) | 1572 | (228) | 3165 | (459) |
| | 2565 | (372) | 1786 | (259) | 1669 | (242) | 1262 | (183) | 3137 | (455) |
| | 2579 | (374) | 1917 | (278) | 1358 | (197) | 1476 | (214) | 2861 | (415) |
| | 2634 | (382) | 1793 | (260) | 1600 | (232) | 1434 | (208) | 3054 | (443) |
| Ambient | 2317 | (336) | 1620 | (235) | 1827 | (265) | 1227 | (178) | 2613 | (379) |
| | 2275 | (330) | 1731 | (251) | 1896 | (275) | 1207 | (175) | 2579 | (374) |
| | 2372 | (344) | 1572 | (228) | 1937 | (281) | 1207 | (175) | 2710 | (393) |
| | 2324 | (337) | 1641 | (238) | 1889 | (274) | 1214 | (176) | 2634 | (382) |
| 450K (+300F) | 1117 | (162) | 979 | (142) | 952 | (138) | 552 | (80) | 359 | (52) |
| | 1117 | (162) | 1062 | (154) | 876 | (127) | 531 | (77) | 1338 | (194) |
| | 1069 | (155) | 876 | (127) | 896 | (130) | 579 | (84) | 862 | (125) |
| | 1103 | (160) | 972 | (141) | 910 | (132) | 552 | (80) | 555 | (124) |

Table 5-8. Longitudinal Compressive Strength of PPO Foam

| Panel No. / Temp. | Strength, kN/m$^2$ (psi) | | | | | | | | | |
|---|---|---|---|---|---|---|---|---|---|---|
| | 72-1U | | 72-3 | | 72-18 | | 72-29 | | 72-32U | |
| 21K (-423F) | 296 | (43) | 159 | (23) | 248 | (36) | 986 | (143) | 1027 | (149) |
| | 310 | (45) | 159 | (23) | 407 | (59) | 917 | (133) | 1110 | (161) |
| | 267 | (39) | 234 | (34) | 283 | (41) | 1000 | (145) | 1145 | (166) |
| | 290 | (42) | 186 | (27) | 310 | (45) | 965 | (140) | 1096 | (159) |
| Ambient | 207 | (30) | 145 | (21) | 179 | (26) | 621 | (90) | 800 | (116) |
| | 207 | (30) | 152 | (22) | 200 | (29) | 641 | (93) | 855 | (124) |
| | 207 | (30) | 145 | (21) | 255 | (37) | 641 | (93) | 855 | (124) |
| | 207 | (30) | 145 | (21) | 214 | (31) | 634 | (92) | 834 | (121) |
| 425K (+300F) | 159 | (23) | 110 | (16) | 103 | (15) | 421 | (61) | 490 | (71) |
| | 145 | (21) | 110 | (16) | 117 | (17) | 441 | (64) | 517 | (75) |
| | 159 | (23) | 103 | (15) | 110 | (16) | 421 | (61) | 524 | (76) |
| | 152 | (22) | 110 | (16) | 110 | (16) | 427 | (62) | 510 | (74) |

| Panel No. / Temp. | Strength, kN/m$^2$ (psi) | | | | | | | | | |
|---|---|---|---|---|---|---|---|---|---|---|
| | 72-34U | | 72-41U | | 72-55 | | 72-60 | | 72-74U | |
| 21K (-423F) | 1365 | (198) | 765 | (111) | 1255 | (182) | 414 | (60) | 2000 | (290) |
| | 1269 | (184) | 883 | (128) | 1131 | (164) | 434 | (63) | 1613 | (234) |
| | 924 | (134) | 807 | (117) | 1379 | (200) | 586 | (85) | 1496 | (217) |
| | 1186 | (172) | 821 | (119) | 1255 | (182) | 476 | (69) | 1703 | (247) |
| Ambient | 855 | (124) | 538 | (78) | 683 | (99) | 234 | (34) | 1041 | (151) |
| | 855 | (124) | 538 | (78) | 827 | (120) | 310 | (45) | 1055 | (153) |
| | 869 | (126) | 538 | (78) | 876 | (127) | 669 | (97) | 986 | (143) |
| | 862 | (125) | 538 | (78) | 793 | (115) | 407 | (59) | 1027 | (149) |
| 425K (+300F) | 524 | (76) | 386 | (56) | 552 | (80) | 159 | (23) | 662 | (96) |
| | 510 | (74) | 358 | (52) | 545 | (79) | 207 | (30) | 648 | (94) |
| | 545 | (79) | 358 | (52) | 476 | (69) | 172 | (25) | 648 | (94) |
| | 524 | (76) | 365 | (53) | 524 | (76) | 179 | (26) | 655 | (95) |

Table 5-9. Transverse Tensile Strength of PPO Foam

| Panel No. / Temp. | Strength kN/m$^2$ (psi) | | | | | | | | | |
|---|---|---|---|---|---|---|---|---|---|---|
| | 72-1U | | 72-3 | | 72-18 | | 72-29 | | 72-32U | |
| 21K (-423F) | 138 | (20) | 97 | (14) | 186 | (27) | 365 | (53) | 427 | (62) |
| | 172 | (25) | 69 | (10) | 179 | (26) | 207 | (30) | 359 | (52) |
| | 172 | (25) | 97 | (14) | 152 | (22) | 255 | (37) | 269 | (39) |
| | 159 | (23) | 90 | (13) | 172 | (25) | 276 | (40) | 352 | (51) |
| Ambient | 193 | (28) | 138 | (20) | 179 | (26) | 310 | (45) | 421 | (61) |
| | 193 | (28) | 138 | (20) | 186 | (27) | 310 | (45) | 310 | (45) |
| | 193 | (28) | 145 | (21) | 172 | (25) | 290 | (42) | 448 | (65) |
| | 193 | (28) | 138 | (20) | 179 | (26) | 303 | (44) | 393 | (57) |
| 425K (+300F) | 117 | (17) | 76 | (11) | 103 | (15) | 338 | (49) | 207 | (30) |
| | 103 | (15) | 69 | (10) | 90 | (13) | 352 | (51) | 186 | (27) |
| | 103 | (15) | 69 | (10) | 83 | (12) | 386 | (56) | 228 | (33) |
| | 110 | (16) | 69 | (10) | 90 | (13) | 359 | (52) | 207 | (30) |

| Panel No. / Temp. | Strength, kN/m$^2$ (psi) | | | | | | | | | |
|---|---|---|---|---|---|---|---|---|---|---|
| | 72-34U | | 72-41U | | 72-55 | | 72-60 | | 72-74U | |
| 21K (-423F) | 303 | (44) | 359 | (52) | 331 | (48) | 455 | (66) | 841 | (122) |
| | 421 | (61) | 310 | (45) | 303 | (44) | 552 | (80) | 552 | (80) |
| | - | - | 317 | (46) | 379 | (55) | 372 | (54) | 524 | (76) |
| | 365 | (53) | 331 | (48) | 338 | (49) | 462 | (67) | 641 | (93) |
| Ambient | 414 | (60) | 338 | (49) | 359 | (52) | 517 | (75) | 600 | (87) |
| | 393 | (57) | 317 | (46) | 400 | (58) | 503 | (73) | 510 | (74) |
| | 386 | (56) | 317 | (46) | 345 | (50) | 490 | (71) | 572 | (83) |
| | 400 | (58) | 324 | (47) | 365 | (53) | 503 | (73) | 558 | (81) |
| 450K (+300F) | 117 | (17) | 179 | (26) | 186 | (27) | 234 | (34) | 221 | (32) |
| | 207 | (30) | 172 | (25) | 214 | (31) | 228 | (33) | 276 | (40) |
| | 179 | (26) | 165 | (24) | 186 | (27) | 221 | (32) | 269 | (39) |
| | 165 | (24) | 172 | (25) | 193 | (28) | 228 | (33) | 255 | (37) |

Table 5-10. Transverse Compressive Strength of PPO Foam

| Temp. \ Panel No. | Strength kN/m$^2$ (psi) | | | | | | | | | |
|---|---|---|---|---|---|---|---|---|---|---|
| | 72-1U | | 72-3 | | 72-18 | | 72-29 | | 72-32U | |
| 21K (-423F) | 41.4 | (6.0) | 13.8 | (2.0) | 151.7 | (22.0) | 53.8 | (7.8) | 133.0 | (19.3) |
| | 27.6 | (4.0) | 10.3 | (1.5) | 81.4 | (11.8) | 64.1 | (9.3) | 39.0 | (5.7) |
| | 17.9 | (2.6) | 11.0 | (1.6) | - | - | 62.7 | (9.1) | 77.0 | (11.2) |
| | 29.0 | (4.2) | 11.7 | (1.7) | 116.5 | (16.9) | 60.0 | (8.7) | 83.0 | (12.0) |
| Ambient | 17.9 | (2.6) | 13.1 | (1.9) | 15.9 | (2.3) | 40.7 | (5.9) | 60.7 | (8.8) |
| | 13.8 | (2.0) | 9.0 | (1.3) | 17.2 | (2.5) | 35.9 | (5.2) | 46.2 | (6.7) |
| | 12.4 | (1.8) | 11.7 | (1.7) | 17.2 | (2.5) | 44.1 | (6.4) | 46.2 | (6.7) |
| | 14.5 | (2.1) | 11.0 | (1.6) | 16.5 | (2.4) | 40.0 | (5.8) | 51.0 | (7.4) |
| 425K (+300F) | 14.5 | (2.1) | 6.2 | (0.9) | 7.6 | (1.1) | 21.4 | (3.1) | 31.7 | (4.6) |
| | 6.9 | (1.0) | 7.6 | (1.1) | 6.2 | (0.9) | 24.1 | (3.5) | 51.0 | (7.4) |
| | 9.0 | (1.3) | 7.6 | (1.1) | 6.9 | (1.0) | 25.5 | (3.7) | 27.6 | (4.0) |
| | 8.3 | (1.2) | 7.6 | (1.1) | 6.9 | (1.0) | 23.4 | (3.4) | 29.6 | (4.3) |

| Temp. \ Panel No. | Strength kN/m$^2$ (psi) | | | | | | | |
|---|---|---|---|---|---|---|---|---|
| | 72-41U | | 72-55 | | 72-60 | | 72-74U | |
| 21K (-423F) | 62.7 | (9.1) | 33.1 | (4.8) | 139.3 | (20.2) | 138.6 | (20.1) |
| | 85.5 | (12.4) | 31.0 | (4.5) | 80.7 | (11.7) | 151.0 | (21.9) |
| | 130.3 | (18.9) | 57.9 | (8.4) | 133.8 | (19.4) | 160.0 | (23.2) |
| | 93.1 | (13.5) | 40.7 | (5.9) | 117.9 | (17.1) | 149.6 | (21.7) |
| Ambient | 53.8 | (7.8) | 44.8 | (6.5) | 106.9 | (15.5) | 116.5 | (16.9) |
| | 47.6 | (6.9) | 43.4 | (6.3) | 49.6 | (7.2) | 111.7 | (16.2) |
| | 50.0 | (7.1) | 55.2 | (8.0) | 105.5 | (15.3) | 100.7 | (14.6) |
| | 50.3 | (7.3) | 47.6 | (6.9) | 86.9 | (12.6) | 109.6 | (15.9) |
| 425K (+300F) | 30.3 | (4.4) | 20.7 | (3.0) | 36.5 | (5.3) | 69.0 | (10.0) |
| | 30.0 | (4.2) | 25.5 | (3.7) | 38.6 | (5.6) | 72.0 | (10.4) |
| | 29.6 | (4.3) | 31.0 | (4.5) | - | - | 73.0 | (10.6) |
| | 29.6 | (4.3) | 25.5 | (3.7) | 37.2 | (5.4) | 71.0 | (10.3) |

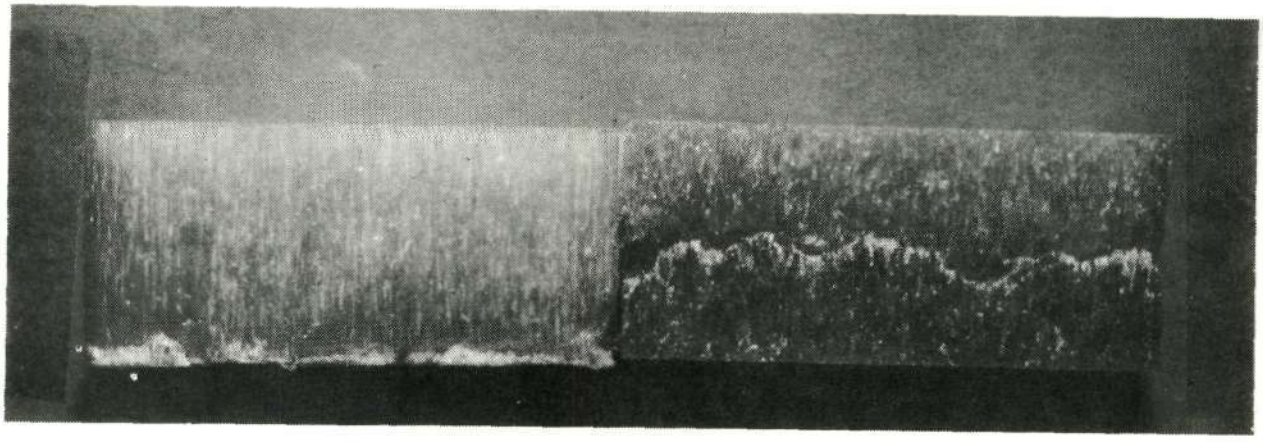

Figure 5-11. Typical Longitudinal Compressive Failures in PPO Foam

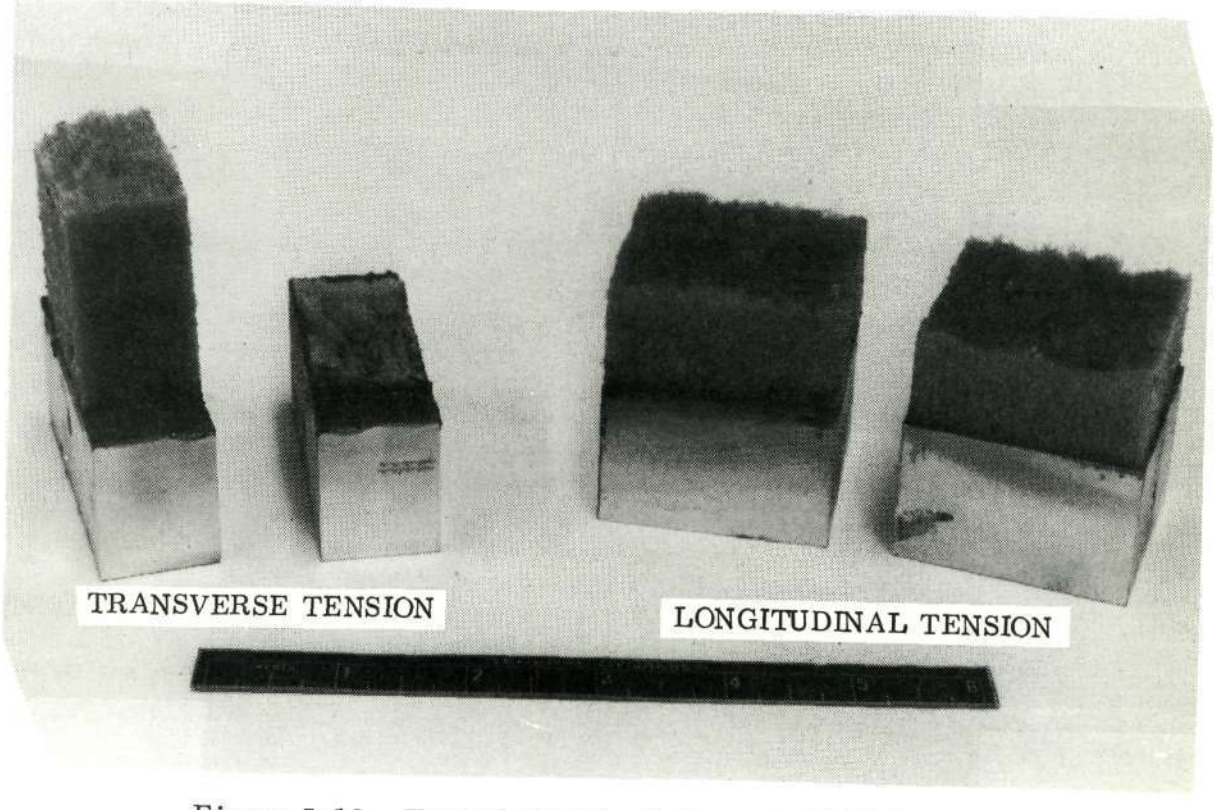


Figure 5-12. Typical Tensile Failures in PPO Foam

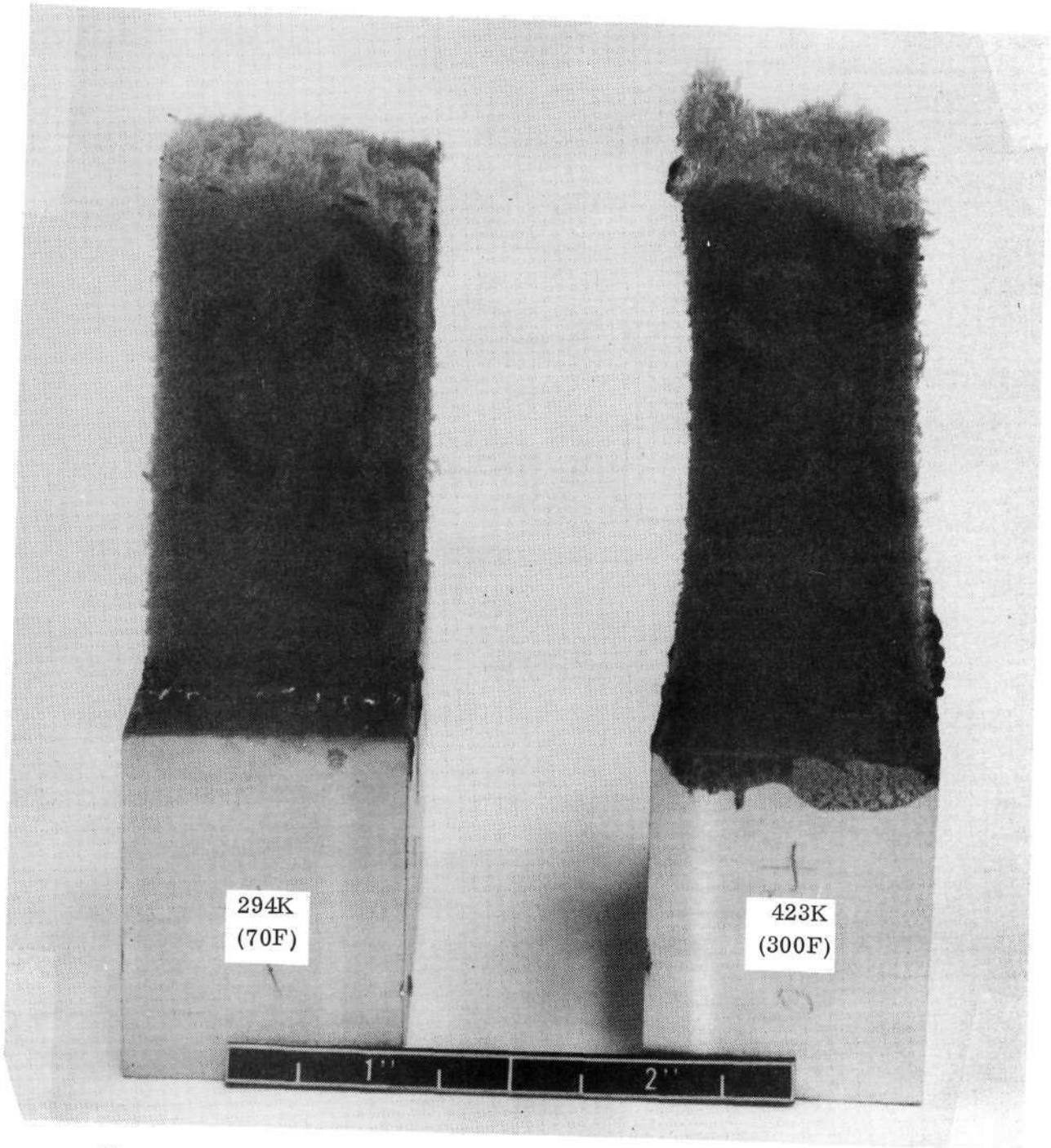


Figure 5-13. Comparison of Transverse Tensile Failure in PPO Foam

Figure 5-14 shows how the strength of PPO foam falls off at high temperatures. The loss of strength decreases as the foam density decreases. In Figure 5-15, the strength of PPO foam at ambient temperature is correlated with the density of the foam. The two low longitudinal strength data points at a density of 50.1 $kg/m^3$ (3.13 $lb/ft^3$) are due to panel 72-60 which had a severely curved cell structure resulting in a drastic reduction in longitudinal strength. Also, the fact that the density variations in the foam test specimens can be as much as 40% results in the scatter of the strength data. Otherwise, the strength of PPO foam increases with increasing foam density.

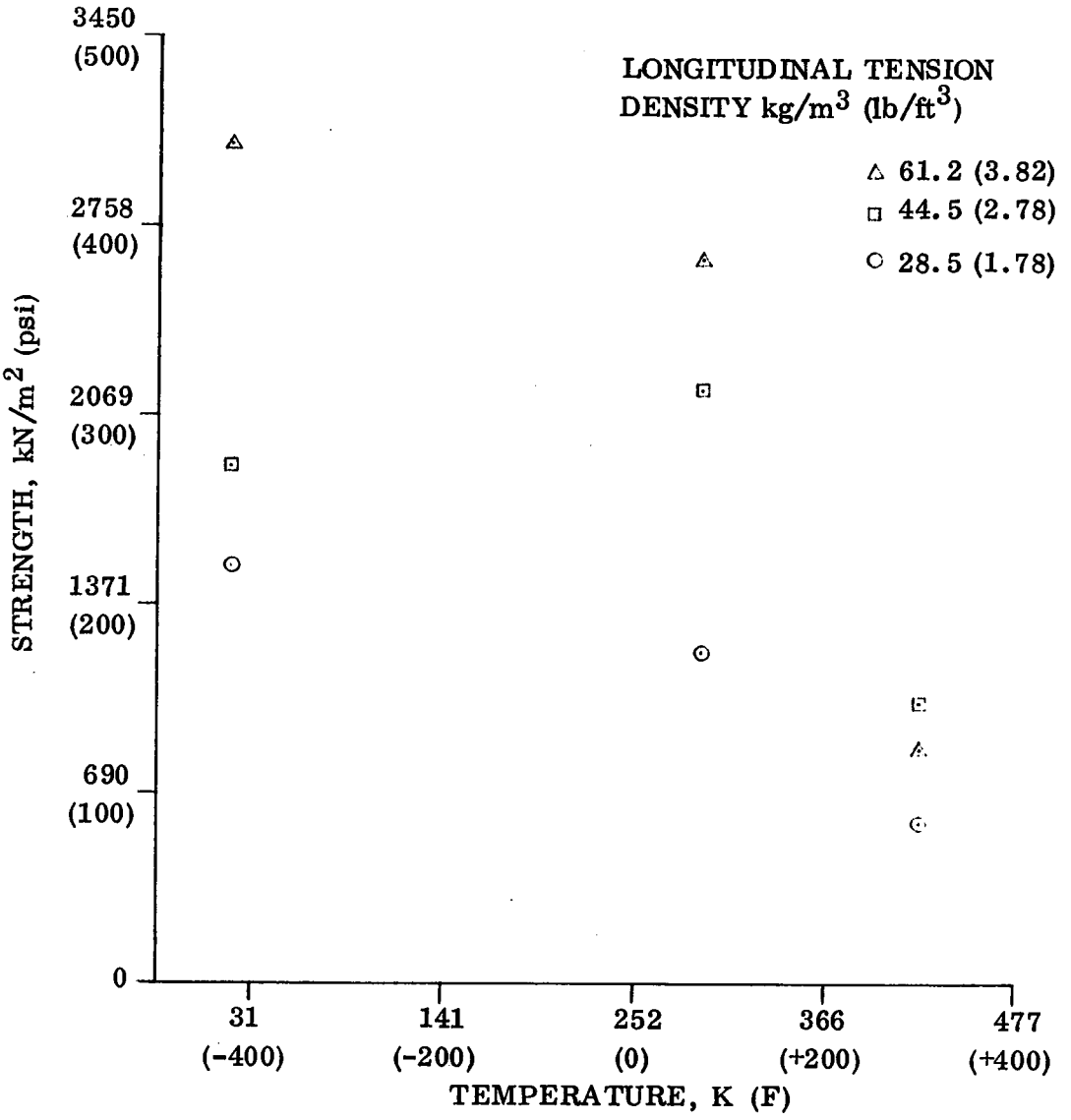


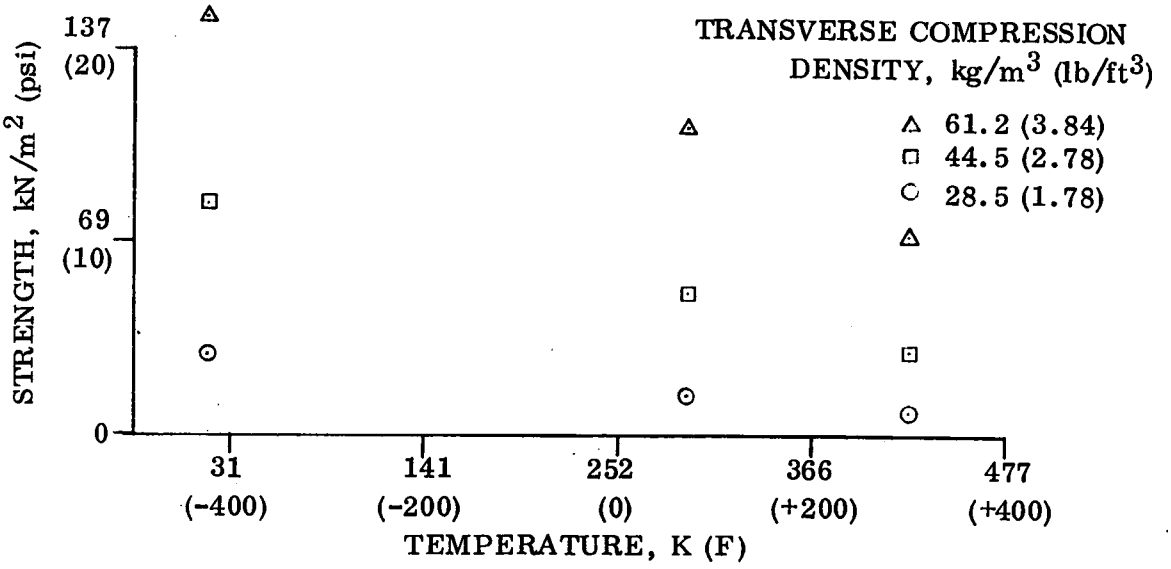


Figure 5-14. Strength of PPO Foam as a Function of Temperature

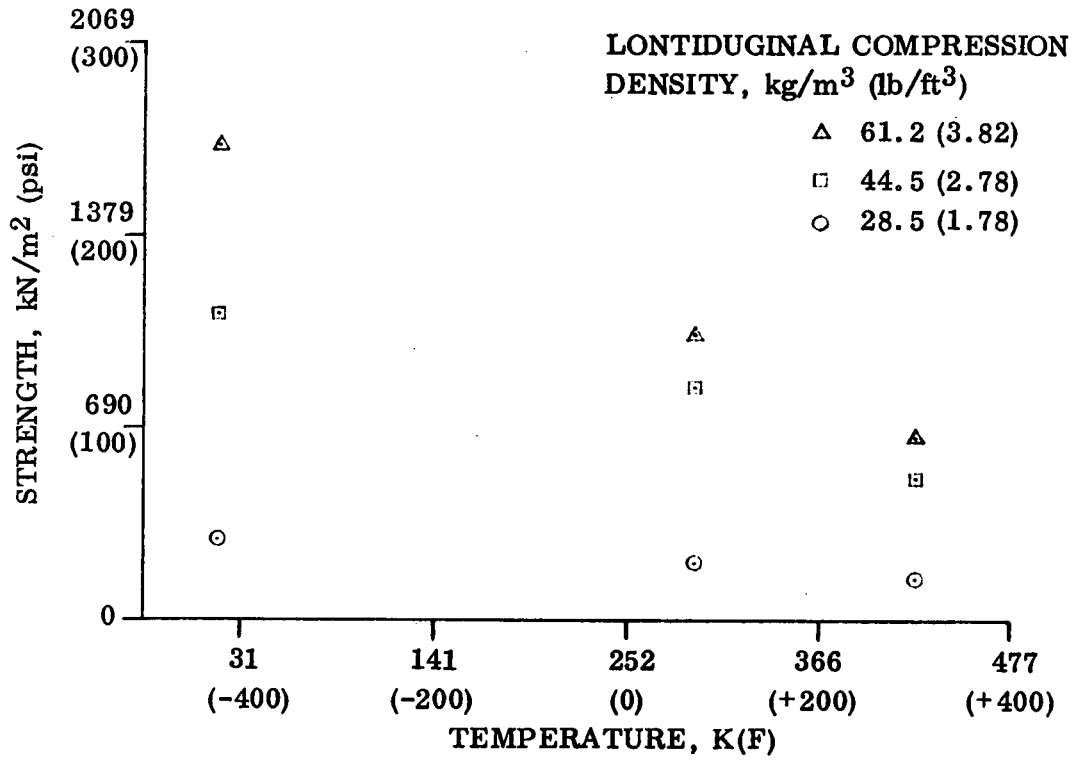


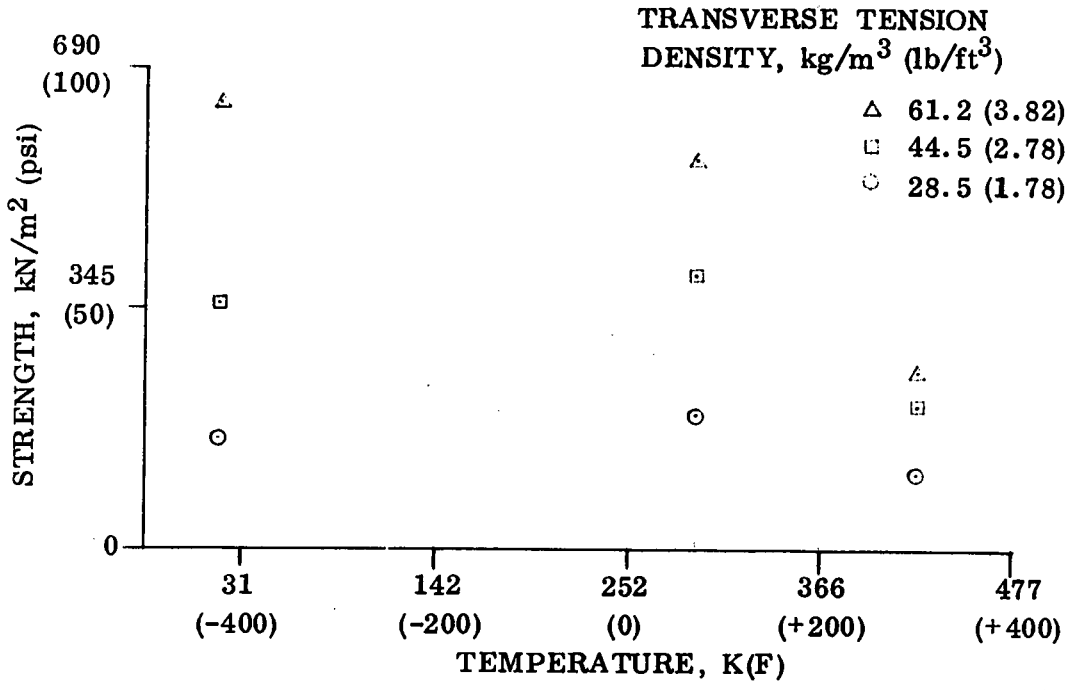


Figure 5-14. Concluded

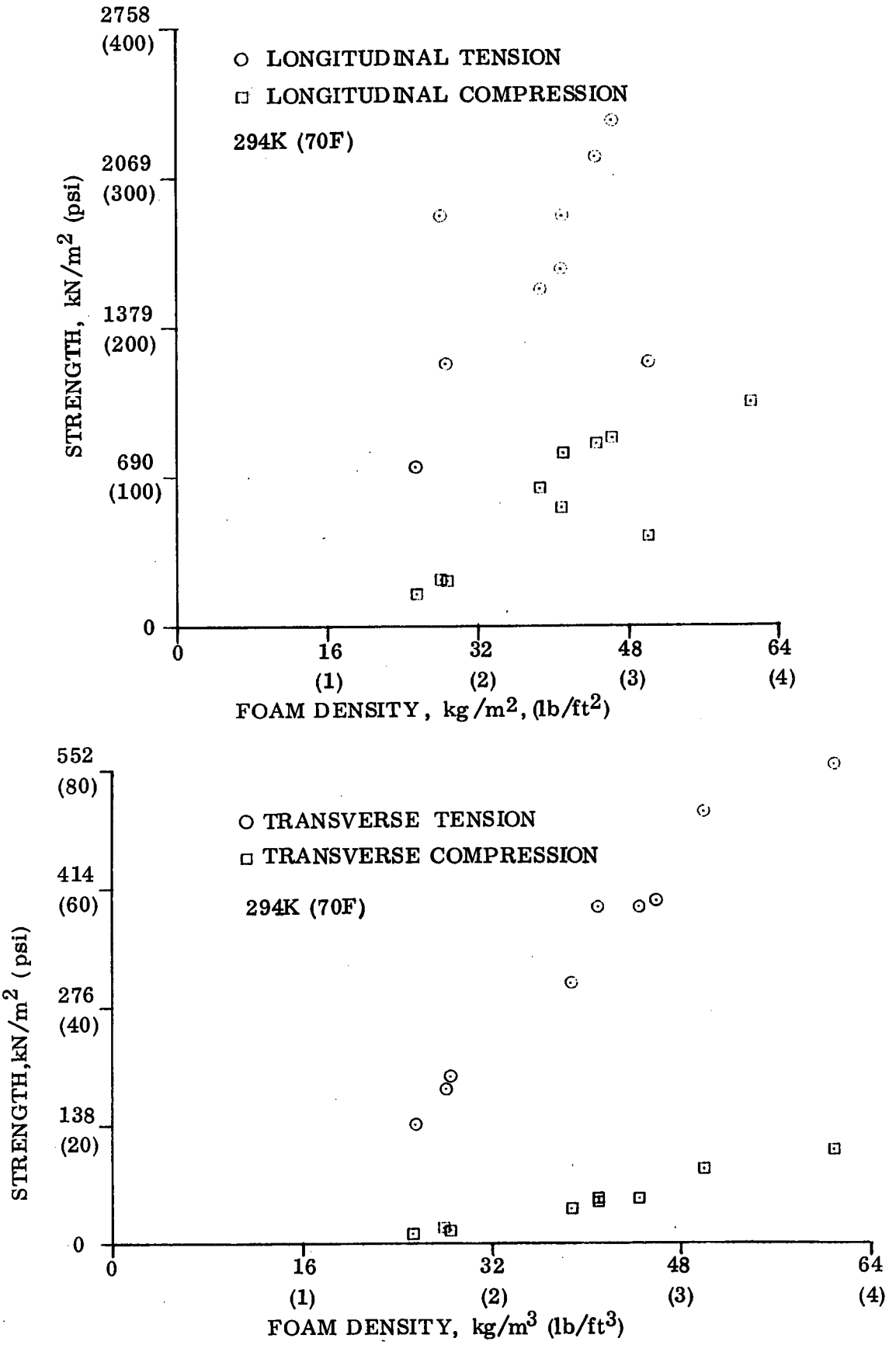


Figure 5-15. Correlation of PPO Foam Strength With Foam Density

## SECTION 6

## PANEL JOINTS (1.4.1)

Various methods of joining PPO foam panels have been considered. Since the available foam panels are approximately one meter square, many panels will have to be jointed together to insulate an $LH_2$ tank. During normal operation of the tankage system, the inner surface of the insulation sees liquid hydrogen temperature (21K (37R)) while the tank surface remains relatively warm, i.e. 200K (360R) to room temperature. At this time, the tank structure experiences maximum strains as a result of pressurizing while the inner surface of the insulation undergoes thermal contractions of approximately one percent. To maintain a reliable joint between panels, either an adhesive bonded joint is required or one providing sufficient residual edge compression to account for the tendency to gap.

The panel joints must not inhibit the insulation by closing off foam cells or by creating heat shorts to the tank skin. Due to the very large number of panel joints involved, the problem of heat shorts could be quite severe. The panel joints must be capable of withstanding the structural and thermal stresses involved in an $LH_2$ tank and be structurally compatible with the foam (no excessive thermal stresses between the joint and the foam). Also, the panel joints must allow the use of practical assembly techniques.

Tongue-and-groove joints and other types of lap joints would involve closing off foam cells, especially if the joints were to be bonded. Closed cells would be subject to pressure cycling and eventual failure. Without bonding the joint, there would be nothing to restrain the lip of a lap joint from pulling up from the surface, leaving gaps and voids in the joint. Bonding a lap joint would create large angular areas of adhesives in the foam which could result in severe thermal stress problems. Finally, since the only requirement of the panel joints is to provide continuity of the foam insulation, the strength of the joint, aside from its own structural integrity, is unimportant, negating any possible structural advantage of a lap joint.

Butt joining the PPO foam panels is very simple and is most compatible with the open-cell insulation system in that a butt joint does not close off the foam cells. The bonded butt joint is a positive joint which can be made during the original installation of the foam without special tooling. Adhesive on a foam butt joint will make the final assembly more difficult at close out panel installation and would be difficult to use with a repair plug since the foam,as it is pressed into place, will tend to scrape the adhesive from the sidewalls and into the bottom of the joint area. The surrounding foam areas would have to be masked to protect them from adhesive that would be scraped off the edge of the panel being installed. In addition, the bonded butt joint

results in a hardpoint discontinuity and associated structural and thermal stresses in the adhesive layer and adjacent foam and presents a heat short through the foam insulation.

PPO foam panels lend themselves to the use of compressive butt joints. The material's low modulus and good ductility in the direction perpendicular to the foam cells allows the panels to be compressed by up to 15 percent without any damage and with good recovery characteristics under room temperature conditions. The compression butt joint offers an easy installation method because adhesive is required only at the face adjacent to the tank wall. This method also avoids any possible heat shorts and structural and thermal stresses in the joint. The unbonded compressive butt joint has been successfully employed in a PPO foam insulation system for an $LH_2$ tank (Ref. 4). The installation method of Reference 4 was to first install alternate foam panels. After the tank wall bond for these panels had cured, the remaining panels were compressed and bonded into their spaces. Before the bond had cured, the compression tooling was removed allowing the panels to expand into place, compressing the previously installed panels. A 2 percent residual edge compression was successfully utilized and tested in this tank system (Ref. 4). The contraction of PPO foam from room temperature to 21K (37R) is about one percent.

A thermal conductivity test specimen of the compression butt joint has been fabricated from one of the best performing configuration screening thermal conductivity test specimens. In this manner, the thermal performance of the joint can be compared directly with the performance of the same specimen without a joint. The specimen used was 72-41; 24.9 mm (0.98 in.) thick. A 127 mm (5.00 in.) hole was cut into the center of the specimen using a rotating cutter, Figure 6-1. The cutter was machined from aluminum and has 0.635 mm (0.025 in.) walls and a smooth, sharp cutting edge. A 25 mm (1.0 in.) arbor machined into the top of the cutter allows the cutter to be mounted vertically. The rotating cutter was used to cut the hole to within 1.27 mm (0.050 in.) of the aluminum foil on the heater. Then the foam in the hole was cut away by hand and the adhesive bond to the aluminum heater was peeled away leaving an extremely clean cut and heater surface.

A 131 mm (5.15 in.) diameter plug was cut from material of the same foam panel as the original thermal conductivity specimen (see Figure 6-2), allowing for a 3 percent residual edge compression. The foam plug was compressed, using the tool shown in Figure 6-3, adhesive applied to the aluminum heater and the bottom of the foam plug and the plug was inserted into the hole. The compression tool was extracted while holding the plug in place. Finally, the specimen was vacuum bagged and left to cure over night. Figure 6-3 shows the finished joint specimen. Except for the ink outline of the hole, the joint is indistinguishable from the original, continuous piece of foam.

The panel joint thermal conductivity specimen will be tested in early September.

Figure 6-1. Panel Joint Specimen and Hole Cutter

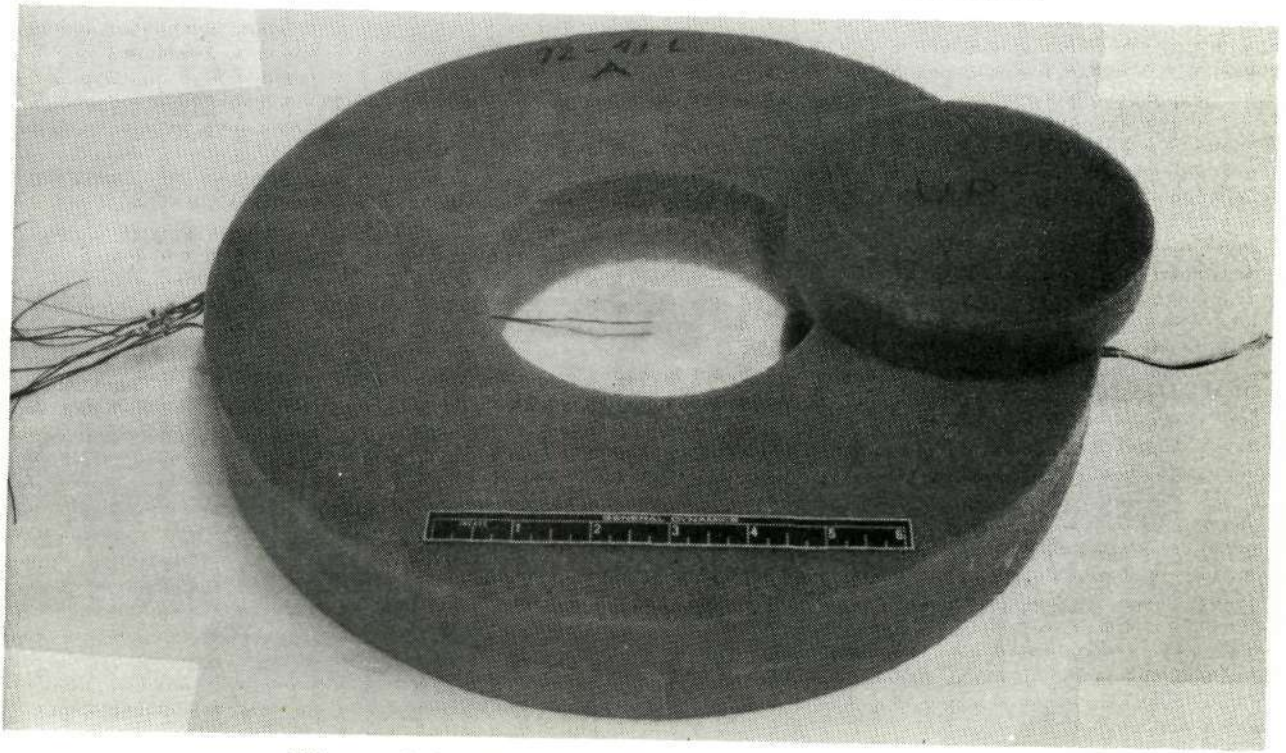

Figure 6-2. Panel Joint Specimen and Foam Plug

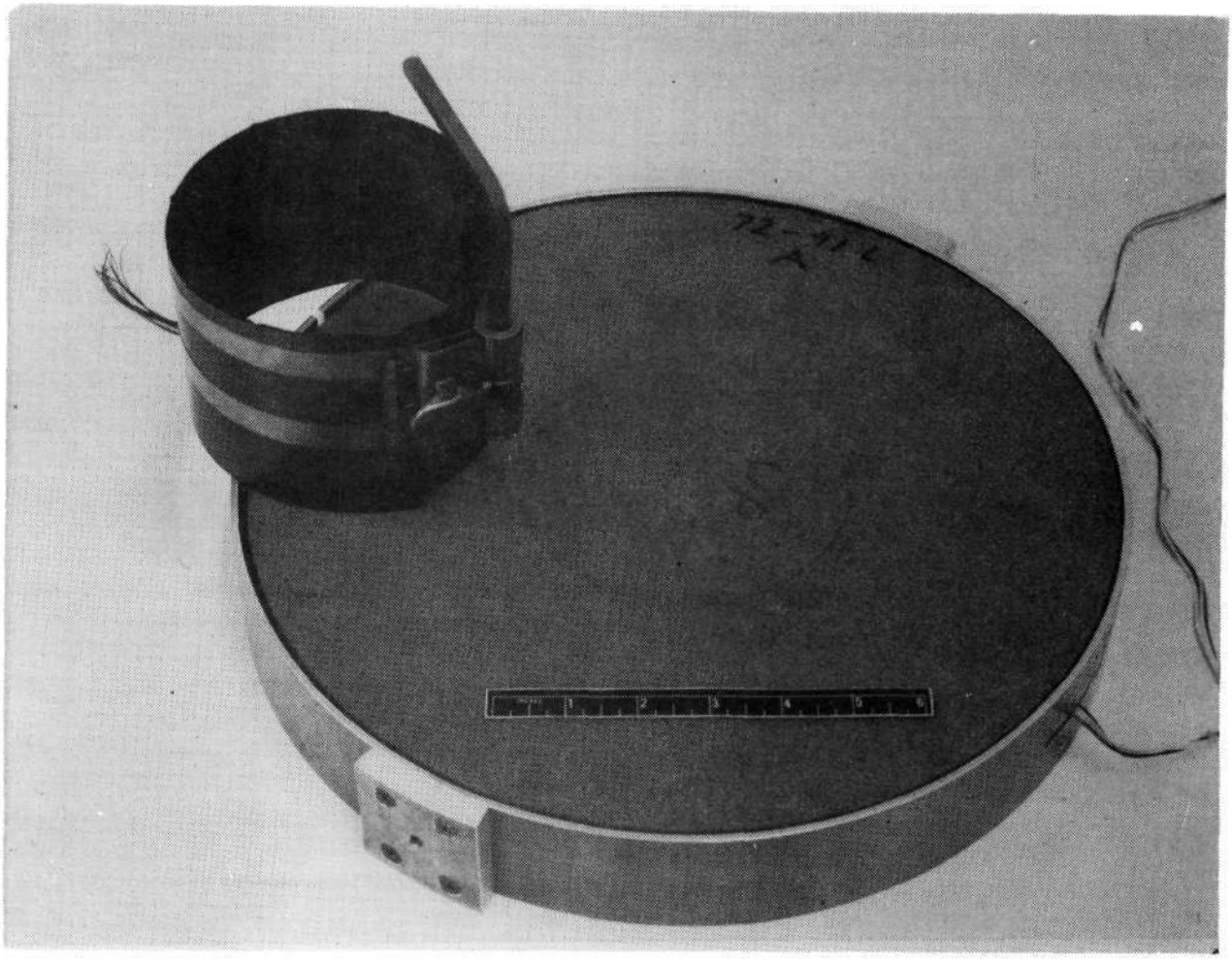

Figure 6-3. Finished Panel Joint Specimen and Foam Plug Compressor

## SECTION 7

## PPO FOAM PROPERTIES INVESTIGATION (2.2)

In order to extend the range of PPO foam configurations considered, two additional panel thicknesses were taken into consideration; a 7.1 mm (0.28 in ) and a 70.0 mm (2.77 in ) thick panel. In this section, thermal conductivity test results are presented for these two configurations along with the results of the previously reported thermal conductivity configuration screening tests (Reference 2). The results of other investigations of the properties of these two configurations are included in their respective sections in this report.

Ten thermal conductivity tests have been performed as part of the PPO foam configuration screening program. The panel numbers, original (manufactured) and test thicknesses and test specimen densities are listed in Figures 7-1 and 7-2. The dashed lines in these figures represent the spread of the conductivity test data for the better formulation screening specimens (Ref. 2).

Comparing the thermal performance of the 14.5 mm (0.57 in ) and 7.1 mm (0.28 in ) panels with the 25.4 mm (1.0 in ) panels (Figures 7-1 and 7-2), as the panel thickness is reduced, the thermal performance worsens. The 14.5 mm specimen has a very poor performance and the 7.1 mm specimen performed so poorly that it was not possible for the heater to bring the hot face temperature above 280K (500R). The minimum effective thickness for this open-cell insulation is between 25.4 mm (1.0 in ) and 14.5 mm (0.57 in ).

Two panels thicker than 25.4 mm (1.0 in ) were tested, a 46.0 mm (1.81 in ) and a 70.0 mm (2.77 in ) panel. The 46.0 mm panel exhibited a performance similar to that of the better 25.4 mm panels. The 70.0 panel also performed as well as the better 25.4 mm panels except at the lowest hot wall temperature, 89 K (160 R) (mean temperature 56 K (100 R)). At this lowest temperature, the $LH_2$-$GH_2$ interface moved into the foam cells, as indicated by thermocouples in the foam, reducing the thickness of the gas layer. Since the effective conductivity of the PPO foam insulation is based upon the total foam thickness, the effective conductivity is increased. In order to efficiently utilize the 70 mm (2.77 in ) panel, the hot wall temperature would have to be increased to about 200 K (360 R) to maintain the $LH_2$-$GH_2$ interface at the foam surface (Figures 7-1 and 7-2).

The effect of an increase in tank pressure on thermal performance of the 7.1 mm (0.28 in) and 70.0 mm (2.77 in) panels was investigated. Table 7-1 gives the results of the pressure rise tests along with the results of the previously tested configuration screening panels (Reference 2). The pressure rise causes the liquid/vapor interface to move

Table 7-1. Effect of Pressure Rise

| Specimen | Avg. Pressure Rise Rate[1] $kN/m^2$/sec (psi/sec) | | Conductivity Increase[2] % | Hot Face Temperature Recovery[2] % |
|---|---|---|---|---|
| 72-74L | 17 | (2.4) | 0 | 100 |
| 72-41L | 20 | (2.9) | 0 | 100 |
| 72-1L | 17 | (2.5) | 0 | 100 |
| 72-64 | 21 | (3.0) | 7 | 94 |
| 72-56 | 25 | (3.6) | 8 | 93 |
| 72-17 | 26 | (3.7) | 64 | 66 |
| 72-30 | 22 | (3.2) | 15 | 89 |
| 72-32L | 19 | (2.7) | 2 | 99 |
| 72-34L | 8.3 | (1.2) | 15 | 71 |
| 72-6 | 0.12 | (0.17) | 62 | 67 |

(1) Between 107 and 276 $kN/m^2$ (15.5 and 40 psia).
(2) Twenty minutes after completion of pressure rise.

into the foam causing an immediate depression in the temperatures. Additional liquid then evaporates increasing the mass of gas in the cells causing the interface to move back toward the surface of the foam. The temperatures then recover to almost their initial values.

Table 7-1 shows the average pressure rise rates and the resulting increase in the thermal conductivity ratio and degree of recovery of the hot face temperature twenty minutes after completion of the pressure rise for all ten configuration screening specimens. The two additional panels, Specimens 72-34L and 72-6 (7.1 mm (0.28 in.) and 70.0 mm (2.77 in.) thick,respectively) performed very poorly in the pressure rise test. The 70.0 mm (2.77 in.) panel shows evidence of severe $LH_2$ intrusion and little temperature recovery even though the pressure rise was quite slow. This may be due to the low quality of the 70.0 mm foam which had a porous low density center layer. When the liquid-gas interface reaches this region, the interface may become unstable, upsetting the gas layer and allowing excessive liquid intrusion.

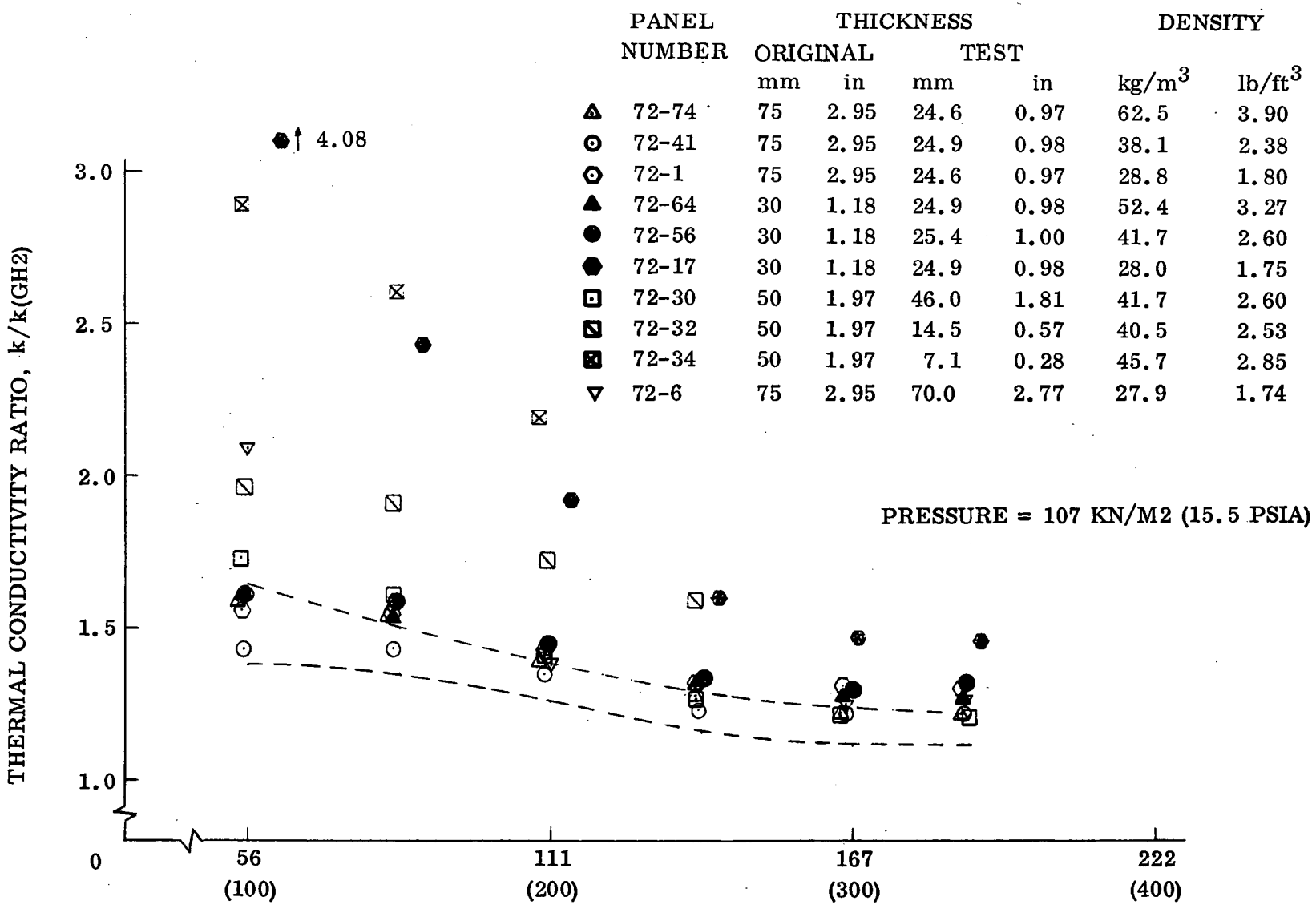


Figure 7-1. Thermal Conductivity in Liquid Hydrogen, Horizontal Orientation - Cells Vertical

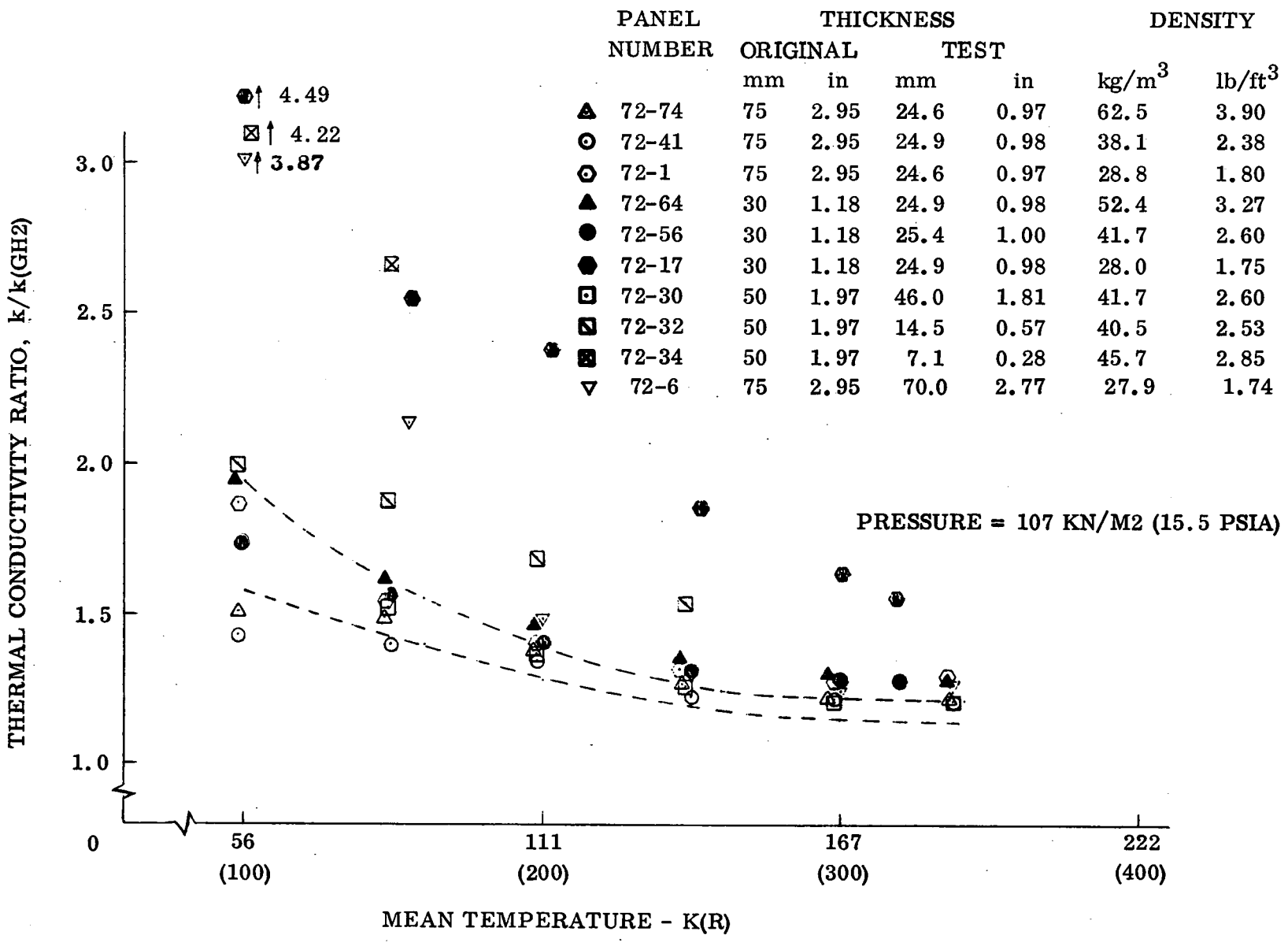


Figure 7-2. Thermal Conductivity in Liquid Hydrogen, Vertical Orientation - Cells Horizontal

## SECTION 8

## NEW TECHNOLOGY

In compliance with the New Technology clause of this contract, personnel assigned to work on the program have been advised, and periodically reminded, of their responsibilities in the prompt reporting of items of New Technology. In addition, response is made to all inquiries by the company-appointed New Technology Representative and copies of reports generated as a result of the contract work are submitted to him for review as a further means of identifying items to be reported. When deemed appropriate, conferences are held with the New Technology Representative to discuss new developments arising out of current work that may lead to New Technology items. The New Technology Representative will be responsible for transmitting New Technology to the Technology Utilization Officer.

Contractor plans to continue New Technology monitoring and surveillance as described above in the ensuing period to assure all items of New Technology are reported as they develop.

## SECTION 9

## REFERENCES


1. "Material Standards and Inspection Specification for PPO Open-Cell Foam Insulation, Preliminary," Convair Aerospace Report 584-4-624, March 1971.

2. "Design and Development of Polyphenylene Oxide Foam as a Reusable Internal Insulation for $LH_2$ Tanks, Phase One Progress Report," Contract NAS8-27566, Convair Aerospace Division of General Dynamics, GDCA 632-1-89, 1 June 1972.

3. Yates, G. B. and F. O. Bennett, "Open-Cell Cryogenic Insulation," Convair Aerospace Division of General Dynamics, GDC-ERR-1586, December 1970.

4. "Space Shuttle Structural Test Program, Final Report - Task 1.1, Cryogenic Tank Structure/Insulation Test," Contract NAS9-10960, Convair Aerospace Division of General Dynamics, GDCA 549-3-092, 25 March 1972.